Published in final edited form as:
Neuroscientist. 2012 December ; 18(6): 567–588. doi:10.1177/1073858411423441.

Structural Remodeling of Astrocytes in the Injured CNS

Daniel Sun[1] and **Tatjana C. Jakobs**[1]
[1]Massachusetts Eye and Ear Infirmary, Harvard Medical School, Boston, MA, USA

Abstract

Astrocytes respond to all forms of CNS insult and disease by becoming reactive, a nonspecific but highly characteristic response that involves various morphological and molecular changes. Probably the most recognized aspect of reactive astrocytes is the formation of a glial scar that impedes axon regeneration. Although the reactive phenotype was first suggested more than 100 years ago based on morphological changes, the remodeling process is not well understood. We know little about the actual structure of a reactive astrocyte, how an astrocyte remodels during the progression of an insult, and how populations of these cells reorganize to form the glial scar. New methods of labeling astrocytes, along with transgenic mice, allow the complete morphology of reactive astrocytes to be visualized. Recent studies show that reactivity can induce a remarkable change in the shape of a single astrocyte, that not all astrocytes react in the same way, and that there is plasticity in the reactive response.

Keywords

protoplasmic; fibrous; reactive astrocytes; review; GFAP; glial scar

Astrocytes are the most abundant nonneuronal cell type within the brain. They are intimately associated with the surrounding neurons and blood vessels, and their processes envelop all cellular components of the CNS. Progress in our knowledge of astrocytes has lagged our understanding of neuronal morphology and function. The reasons may be that astrocytes have traditionally been thought of as simply filling in the spaces between neurons and that they do not generate action potentials. We have learned much about the functional diversity of neurons with different morphologies, but we are only beginning to discover the complex and diverse roles of astrocytes.

Astrocytes contact blood vessels and make gap junction connections with other astrocytes and oligodendrocytes. They support activities essential for neuronal function, including promoting synapse formation, regulating the extracellular concentrations of ions and neurotransmitters, providing metabolic substrates for neurons, coupling blood flow to neuronal activity, and maintaining the blood-brain barrier (Ullian and others 2001; Simard and Nedergaard 2004; Iadecola and Nedergaard 2007; Pellerin and others 2007; Rouach and others 2008; Robel and others 2011). Central questions are whether all astrocytes or just specific types share these functions and what the relevance is of these differences to human disease.

Corresponding Author: Daniel Sun, Massachusetts Eye and Ear Infirmary, Department of Ophthalmology, 243 Charles Street, Boston, MA 02114, daniel_sun@meei.harvard.edu.

Declaration of Conflicting Interests
The author(s) declared no potential conflicts of interest with respect to the research, authorship, and/or publication of this article.

Astrocytes alter their morphology in pathological states. While studying brains from patients with multiple sclerosis, Carl Frommann described pathological glial cells in general as larger and having fewer processes compared to normal glia. He also noted that glial cells were still present in areas of fiber degeneration. In 1910, Alois Alzheimer concluded that any type of pathology is accompanied by a glial response. We now know that astrocytes respond to multiple forms of CNS insult (trauma, ischemia, infection, inflammation, neurodegeneration) by becoming "reactive," changing their morphology, physiology, function, and gene expression. This response is graded; depending on the nature and severity of the insult, there is a continuum of progressive alterations.

In this review, we focus on the morphological remodeling of reactive astrocytes. Although the reactive phenotype was first suggested more than 100 years ago based on morphological changes, some simple but fundamental questions remain. What does an individual reactive astrocyte look like? Do all astrocytes remodel in the same way, and do all insults produce the same effect? The ability of reactive astrocytes to remodel and form a glial scar that impedes axon regeneration led to an overall negative connotation of the effects of reactivity. Recent work, however, reveals that they can also play a beneficial role (Sofroniew 2009; Sofroniew and Vinters 2010). We do not know how a population of these cells reorganizes to form the glial scar. How long do these changes last? We begin by describing the normal morphology and spatial organization of astrocytes in the gray and white matter and then discuss how they remodel after insult.

Morphological and Functional Heterogeneity

From the late 19th century, astrocytes had already been divided into two main subtypes, protoplasmic or fibrous, based on the differences in their morphology and anatomical locations. Protoplasmic astrocytes are located in the gray matter and fibrous astrocytes in the white matter. These two main categories retain their validity and usefulness today. Other morphologically distinct forms of astrocytes that were recognized early are the Müller cells in the retina and Bergmann glia in the cerebellum. Since then, many other less numerous and more regional populations of astrocytes have been described, such as velate astrocytes, perivascular astrocytes, marginal glia, tanycytes, and various forms of ependymal glia (e.g., ependymocytes, choroid plexus cells, and retinal pigment epithelial cells) (Reichenbach and Wolburg 2009).

An important implication of this diversity is that we can no longer consider astrocytes as a homogenous group of cells. A function observed in one type of astrocyte may not necessarily be observed in other types. Because of their prevalence, studies have, to date, focused on protoplasmic and fibrous astrocytes, Müller cells, and Bergmann glia. Moreover, these studies are confined to certain regions of the CNS: the cortex, hippocampus, cerebellum, spinal cord, retina, and optic nerve. We still know little about other astrocytes in other regions of the brain.

Much of the morphological diversity of astrocytes is determined by the structural and functional interactions of the astrocyte with its microenvironment, particularly during development, as the processes form specialized contacts with neighboring blood vessels, axons, synapses, the pia, and/or other cell bodies (Sobue and Pleasure 1984; Hatten 1985). Emsley and Macklis (2006) demonstrated that not only the morphology but also the density and proliferation rates of astrocytes are each factors that can independently define different regions of the brain. Therefore, regional astrocyte heterogeneity may reflect important molecular and functional differences between types of astrocytes, much like the long-accepted heterogeneity of neuronal populations.

Expression of glial fibrillary acidic protein (GFAP) has become the prototypical marker for the immunohistochemical identification of astrocytes within the CNS (Box 1). Its expression pattern differs across the CNS. In the cortex and hippocampus, GFAP labeling of protoplasmic astrocytes reveals the typical star-shaped appearance of astrocytes (Fig. 1A) and, in the cerebellum, a radial appearance. In the optic nerve, astrocytes are organized so densely that labeling for GFAP simply shows a meshwork of processes, making it impossible to discern their boundaries (Fig. 1B). Yet, this is not observed in another white matter region, the corpus callosum. Here, GFAP-labeled astrocytes are well separated from one another and do appear stellate (Fig. 1C). Similiar to those in the optic nerve, retinal astrocytes labeled with GFAP show no separation (Fig. 1D). There are at least four distinct morphologies of GFAP-positive cells within the human and chimpanzee cortex (inter-laminar, varicose projecting, protoplasmic, fibrous) (Fig. 1E–G) compared with two in the rodent (protoplasmic, fibrous). In contrast, the cortex of lower order primates, including the rhesus macaque and squirrel monkeys, contains three subtypes of astrocytes (Oberheim and others 2009).

Astrocytes show heterogenous expression of many ion channels and neurotransmitter receptors, similiar to neurons. These differences create diversity in their electrophysiological responses (membrane potential and conductance) and Ca^{2+} dynamics (Parpura and Haydon 2009). Although astrocytes have not been traditionally classified based on their physiological properties, several studies have described electrophysiologically “complex” and “passive” astrocytes (Müller and others 1992; Steinhäuser and others 1992; Chvatal and others 1995; Pastor and others 1995). Astrocytes also differ in their expression of gap junctions and the extent of coupling (Lee and others 1994; Blomstrand and others 1999), and the connectivity of astrocytic networks is highly specific (Sul and others 2004; Houades and others 2008). These differences have been reported for astrocytes in different brain regions as well as for astrocytes within the same brain region. Recent studies have begun to suggest that heterogeneous populations of protoplasmic astrocytes may exist within hippocampal CA1 (Jabs and others 1997; D’Ambrosio and others 1998; Walz and Lang 1998; Walz 2000).

Besides the well-studied difference in function between protoplasmic and fibrous astrocytes, it is unknown whether all astrocytes possess the same functional capabilities. Are there subtypes with distinct functions? For example, different populations of astrocytes differ in their ability to take up extracellular glutamate; some astrocytes from the hypothalamus lack glutamate uptake currents (Drejer and others 1982; Israel and others 2003). Cultured astrocytes from different brain regions have different capacities in stimulating neurite growth and branching (Denis-Donini and others 1984; Garcia-Abreu and others 1995). They also differ in their permissivity to neuronal migration. Astrocytes in the respiratory nuclei of the brain stem have a specialized ability to sense pH changes and can control breathing through pH-dependent ATP release (Gourine and others 2010). Radial glia-like cells exist in the subependymal zone at the lateral wall of the lateral ventricle and in the dentate gyrus of the hippocampus that can act as stem cells (Robel and others 2011).

What is the relevance of these differences to human disease? Yeh and others (2009) suggested that regional molecular heterogeneity of astrocytes may underlie the predominance of tumors in children to be found in certain brain locations. Two thirds of brain tumors in individuals with neurofibromatosis type 1 (NF1) arise in the optic pathway. They found that expression of the brain tumor suppressor gene NF1 was decreased in neocortical astrocytes relative to other brain regions. This correlated with increased cell proliferation in the optic nerve, but not neocortex, following NF1 inactivation in vitro and in vivo.

It is very important to remember that GFAP labeling gives an incomplete view of an astrocyte. With the introduction of single cell dye injections, particle-mediated dye transfer, and transgenic mice (Box 1), the complete morphology of individual astrocytes and their spatial organization can be better studied. These techniques reveal an immense diversity in the morphology of astrocytes that was not apparent with GFAP labeling. For example, protoplasmic and fibrous astrocytes may appear quite similiar upon GFAP labeling (compare Fig. 1A with 1C) but are distinctly different when their full morphology is visualized (Fig. 2A).

Protoplasmic Astrocytes

Protoplasmic astrocytes are the most abundant astrocyte population in the gray matter and the best studied in terms of their morphology and organization. They are bushy or spongiform in nature with approximately 5 to 10 primary processes that spread more or less radially from the soma. From these processes, very dense ramifications of fine processes extend to enwrap synaptic connections and impart a distinct boundary to the spatial territory of each astrocyte (Kosaka and Hama 1986; Bushong and others 2002; Ogata and Kosaka 2002; Wilhelmsson and others 2006; Oberheim and others 2008, 2009) (Fig. 2B). At least one of the processes contacts blood vessels via perivascular endfeet. Although protoplasmic astrocytes typically occupy a spherical region of neuropil (e.g., in the cortex), their morphology can vary slightly between various gray matter regions. For example, astrocytes in CA1 stratum radiatum are fusiform in shape, with their long axis oriented parallel to the descending apical dendrites of CA1 pyramidal cells (Bushong and others 2002) (Fig. 2C).

The volume of neuropil an astrocyte occupies in the rodent brain has been reported to range from 14,700 to 22,906 μm^3 in the cortex to 65,900 to 85,300 μm^3 in the hippocampus (Bushong and others 2002; Ogata and Kosaka 2002; Chvatal and others 2007; Halassa and others 2007). The size of protoplasmic astrocytes in different species has so far been found to parallel the increase in complexity of higher brain functions (e.g., humans v. nonhuman primates v. rodents). Human protoplasmic astrocytes are 2.55-fold larger in diameter and have processes that are 2.6-fold longer, 1.3-fold thicker, and 10-fold more GFAP immunoreactive than rodent protoplasmic astrocytes (compare Fig. 2D with Fig. 1A; Table 2). These dimensions result in a 16.5-fold increase in astrocytic volume (Oberheim and others 2008, 2009). Protoplasmic astrocytes in nonhuman primates manifest an intermediate phenotype between rodents and humans: they are smaller and less complex than human astrocytes but larger and more complicated than those seen in rodents.

Protoplasmic Astrocytes Are Organized in Nonoverlapping Spatial Domains, Whereas Fibrous Astrocytes Are Not

The spatial organization of protoplasmic astrocytes has been primarily studied in the cortex and hippocampus. Using single cell dye injections to label astrocytes, numerous studies show that neighboring protoplasmic astrocytes tile in nonoverlapping spatial domains, with very limited overlap of neighboring processes (Bushong and others 2002; Ogata and Kosaka 2002; Wilhelmsson and others 2006; Halassa and others 2007) (Fig. 2E). This organization is proposed to be brought about by contact spacing (Chan-Ling and Stone 1991; Tout and others 1993; Bushong and others 2002). Such an arrangement is established in the early postnatal period in parallel with neuronal and vascular territories. The fact that these domains are most clearly defined in areas of high synaptic density, such as the cortex and hippocampus, suggests that this organization might be important for astrocytes to modulate synaptic transmission. In the rodent cortex, one astrocyte domain can encompass 4 to 8 neuronal somata, 300 to 600 dendrites, and approximately 140,000 synapses (~2,000,000 synapses in human brain) (Bushong and others 2002; Oberheim and others 2006; Halassa and others 2007).

Based on this organization, a single domain may represent a functional unit, whereby the synapses, blood vessels, and neurons within are under the control of a single astrocyte. Such synaptic modulation could be independent of and in addition to neuronal networking. An astrocyte has the potential to coordinate small clusters of neurons if signals are propagated directly between an astrocyte and neuronal cell bodies (e.g., glutamate/ATP release) (Angulo and others 2004; Fellin and others 2004; Kozlov and others 2006), whereas when signals are transmitted from the processes of astrocytes to dendrites/spines/synapses, one astrocyte has the potential to modulate the function of hundreds of neurons with spatially dispersed somata (Fig. 2F). There is an additional layer of organization. The processes of a single neuron can extend into the domain of several astrocytes, and thus, different compartments of the neuron can be affected by different astrocytes (Fig. 2G). Elucidating the domain organization has provided a structural basis for the functional interaction between neurons and astrocytes. However, the functional significance of this organization or the consequences of its loss following injury or disease remains to be fully understood.

Fibrous Astrocytes

Fibrous astrocytes are morphologically distinct from protoplasmic astrocytes. They are less complex and have fewer GFAP immunoreactive processes (Fig. 1C). They reside in white matter fiber tracts such as the spinal cord, corpus callosum, retinal nerve fiber layer, and optic nerve. Their somas are often evenly spaced and arranged in rows between the axon bundles. This spacing is likely attributable to the structural support they provide for the axon tracts. They have thick primary processes oriented in parallel to the axons and are much longer than protoplasmic astrocytes; some can be up to 300 μm long (in the optic nerve, they may extend 200–500 μm long) (Fig. 3A). These processes have none of the numerous fine processes making up the spongiform appearance characteristic of protoplasmic astrocytes. The primary processes can be smooth, rough, straight, or undulating (Sun and others 2009). They vary in the degree of higher order branching, with some showing many short fine offshoots (Fig. compare 3A and 3B). In most cases, the bulbous endfeet of a primary process establishes several perivascular and/or subpial contacts. These astrocytes send numerous finger-like outgrowths (perinodal processes) that contact axons at nodes of Ranvier (Raine 1984; Waxman and Black 1984; Butt and others 1994c). Human fibrous astrocytes are larger than those of mice, with an average GFAP-defined domain diameter of 183.2 ± 6.1 μm compared to 85.6 ± 2.7 μm in mice (Oberheim and others 2009) (compare Fig. 1C with Fig. 3F and 3G).

Fibrous astrocytes show much greater variation in morphology both between and within the same CNS structures than protoplasmic astrocytes. For example, fibrous astrocytes in the rodent optic nerve have three dominant forms based on the orientation of their primary processes with respect to the long axis of the nerve: random, transverse, and longitudinal forms (Butt and others 1994a, 1994b; Sun and others 2009) (Fig. 3A–3D). Astrocytes within the unmyelinated optic nerve head region are only of the transverse form (Fig. 3E). The transversely and longitudinally oriented astrocytes may represent extreme variants of the random form (Butt and others 1994a, 1994b; Sun and others 2009). It is unknown whether these morphologically distinct forms have different functional/molecular differences, such as reported for gray matter astrocytes in the hippocampus and oligodendrocyte precursor glial cells (Steinhaüser and others 1992; Zhou and Kimelberg 2001; Bachoo and others 2004; Wallraff and others 2004; Karadottir and others 2008).

Fibrous astrocytes do not occupy individual spatial domains (Fig. 3H). They occupy a variable volume of neuropil, and the processes of neighboring astrocytes overlap extensively. This may relate to their presence in axonal fiber tracts rather than being in

synapse-containing neuropil. This supports the idea that these astrocytes have an important supporting or metabolic role rather than modulating neuronal function.

Remodeling of Astrocytes in the Normal (Uninjured) CNS

Astrocytes play a role in the maintenance of the extracellular concentration of neuroactive substances and the volume of extracellular space. All transmembrane ionic shifts (e.g., Na^+, K^+, Ca^{2+}, H^+) and membrane transport mechanisms such as glutamate uptake are followed by water movement. Fluctuations in the level of extracellular neurotransmitters or ions during neuronal activity or pathology can thus activate astrocyte regulatory volume changes, resulting in the shrinkage or swelling of astrocytes (Sykova 2004; Chvatal and others 2007; Benesova and others 2009; Risher and others 2009). These changes are reviewed below in the section “Reactive Astrocytes.”

At the ultrastructural level, the processes of astrocytes in physiological conditions continously modify their association with dendritic spines and synapses. This morphological remodeling occurs over minutes and consists of gliding of thin lamellipodia-like processes as well as process extension and retraction (Hirrlinger and others 2004; Haber and others 2006). Many of these spine-astrocyte interactions are transient. Approximately 57% of hippocampal synapses are juxtaposed with astrocytic processes at any given time (Ventura and Harris 1999). Remarkably, the processes of astrocytes are more motile than their dendritic spine counterparts.

Process remodeling has also been linked to synaptic activity and behavior. For example, long-term potentiation increases the surface area of the astrocyte process enwrapping a synapse and the number of synapses receiving astrocyte coverage (Lushnikova and others 2009). Similiar changes are found in electron microscopy studies of the visual cortex of rats raised in a complex environment (Jones and Greenough 1996; Soffie and others 1999) and in the somatosensory cortex of mice subjected to 24 hours of whisker stimulation (Genoud and others 2006).

Naturally occuring changes in the processes of astrocytes and dendrites also occur during the estrous cycle. Dendritic spine density is increased on pyramidal cells (Woolley and others 1990), whereas astrocyte volume becomes lower in area CA1 of the hippocampus during proestrus, a time when estrogen levels peak during the reproductive cycle (Garcia-Segura and others 1994; Klintsova and others 1995; Viola and others 2009). Astrocytes also display a structural response to glutamate by increasing the number of surface filapodia (Cornell-Bell and others 1990). Astrocytes modulate synaptic efficacy of magnocellular neurons of the supraoptic nucleus of the hypothalamus by extending and retracting their processes. This remodeling occurs during lactation, pregnancy, and episodes of dehydration and coincides with differential neuronal firing patterns (Panatier and Oliet 2006).

The remodeling of processes may serve several functions: it may regulate the positioning of key molecules (e.g., glutamate transporters) that actively control the properties of the synaptic microenvironment (Huang and Bergles 2004). This would control the degree of glutamate spillover onto neighboring synapses and modify heterosynaptic plasticity (Kullmann and Asztely 1998). This is in addition to the ability of astrocytes to partition the extracellular space and influence the diffusion of neuroactive substances (Sykova 2004). The positioning and morphological rearrangement of processes may also serve to correctly place the glial machinery for vesicular-mediated release of glutamate, ATP, and D-serine in response to synaptic activity (Bezzi and others 2004; Zhang and others 2004; Mothet and others 2005; Pascual and others 2005). In addition, the motility can directly shape the neuronal environment. Localized expression of the glycosylphosphatidylinositol (GPI)–anchored glycoprotein ephrin-A3 on astrocyte processes at synapses activates the

neighboring tyrosine kinase receptor EphA4 on dendritic spines, thereby stabilizing their structure (Murai and others 2003).

Morphological Changes of Individual Reactive Astrocytes

Despite the long-standing recognition that astrocytes have the potential to undergo reactive changes, and in spite of their ubiqutious presence at sites of CNS pathology, we still know very little about their behavior in general and even less in specific diseases. We have no consensus on a definition or model of what reactivity is. What set of characteristics distinguish a reactive astrocyte from a normal astrocyte? Is the up-regulation of GFAP and hypertrophy alone sufficient to consider an astrocyte reactive? Early characterizations of the reactive phenotype were derived from morphological work based on labeling with GFAP, so we still do not know what an individual reactive astrocyte looks like, how a population forms the glial scar, and whether these morphological changes are reversible. The molecular triggers, modulators, and signaling pathways involved in astrocyte reactivity are reviewed elsewhere (Ridet and others 1997; Logan and Berry 2002; Sofroniew 2009; Buffo and others 2010; Kang and Hebert 2011). Here, we review the morphological changes of individual reactive astrocytes, first from studies using GFAP labeling and then from studies that visualize astrocytes in their entirety. We then discuss how reactive astrocytes as a population reorganize to form the glial scar.

GFAP Labeling

The up-regulation of intermediate filament proteins, in particular GFAP and vimentin, by reactive astrocytes is perhaps the best known hallmark of reactivity. This is accompanied by the characteristic hypertrophy of the cell body and processes. These changes have been observed following many types of injuries, including mechanical trauma, ischemia/hypoxia, inflammation, neurodegeneration, and in virtually all locations throughout the CNS (Eng and others 2000; Pekny and Nilsson 2005; Sofroniew and Vinters 2010; Middeldorp and Hol 2011) (Fig. 4A and 4B).

Here, we focus on recent studies that have performed morphometric analysis on GFAP labeling, measuring the total diameter of labeled astrocytes, the length of the longest process, the diameter of the thickest process, and the number of main processes emanating from the soma (Wilhelmsson and others 2004; Oberheim and others 2008, 2009; Rodriguez and others 2009; Sun and others 2010). From these quantifications, the universal characteristic of reactivity is the hypertrophy of the cell body and processes. The other morphometric parameters, which primarily relate to the processes, change depending on many factors such as the type of insult, its severity, and the location of the astrocyte in relation to the core of the lesion.

Protoplasmic and fibrous astrocytes respond to mechanical trauma by thickening their cell body and processes. In the cortex and hippocampus, the thickness and length of GFAP-labeled processes increase by up to two-fold (Wilhelmsson and others 2004). In an optic nerve crush model, there was a peak 0.5-fold increase in the thickness of processes at 3 and 7 days postcrush, which then returned to normal levels by 2 weeks (Sun and others 2010). Intermediate filaments are important in developing the reactive morphological changes. Reactive astrocytes devoid of both GFAP and vimentin ($GFAP^{-/-}Vim^{-/-}$), but not GFAP ($GFAP^{-/-}$) or vimentin ($Vim^{-/-}$) alone, show very limited hypertrophy of the cell body and processes (Pekny and others 1999; Wilhelmsson and others 2004).

Reactive cortical astrocytes in models of epilepsy and Alzheimer disease increase the expression of GFAP, but only in epilepsy do the parameters of the processes change (Oberheim and others 2008). Epilepsy causes a 2- to 2.5-fold increase in the thickness and

length of the longest process, lasting for the duration of the study (6 months). However, the number of GFAP-positive processes remain constant. In another study of Alzheimer disease, Rodriguez and others (2009) found that reactive astrocytes atrophied, reducing the number of processes and overall decreasing both the surface area and volume of GFAP-labeled structures. This effect was observed for astrocytes positioned away from the amyloid plaques. Astrocytes directly surrounding amyloid plaques display the typical reactive characteristics.

Caution must be taken in intepreting results from studies that use GFAP to label reactive astrocytes. GFAP does not reveal the true morphology of an astrocyte, and many astrocytes do not express GFAP at immunohistochemically detectable levels. For example, the elongation of GFAP-labeled processes seen when a protoplasmic astrocyte becomes reactive appears to increase the volume of neuropil an astrocyte occupies. Using single cell dye injection, Wilhelmsson and others (2006) demonstrated that, at least after mechanical trauma, this is not the case (see section “The Spatial Organization of Reactive Protoplasmic Astrocytes Following Injury and Disease”). In addition, there has been a tendency to overestimate the contribution of astrocyte proliferation in the reactive process. The up-regulation in GFAP and hypertrophy can lead to the false impression of an increase in astrocyte numbers because more astrocytes are immunohistochemically detectable and the large astrocytes seem more densely packed (Sofroniew and Vinters 2010).

Although it has been known for a long time that astrocytes change shape following injury, only recently has their shape been fully reconstructed in three dimensions and the morphological changes quantified. Many of these studies assess protoplasmic astrocytes of the cortex or hippocampus. Less is known about the behavior of fibrous astrocytes in the white matter.

The reaction of astrocytes to insult is spatially distinct: astrocytes adjacent to the core of a lesion react differently from those further away. This difference applies to both the morphological and functional reaction. For example, one factor that determines whether reactive protoplasmic astrocytes maintain their nonoverlapping spatial domain appears to be the location (see below). Also, during the initial response to insult, a reactive astrocyte adjacent to the core of a lesion may have a beneficial role in preventing degeneration of surrounding tissue, whereas one at a more distant location may have a deleterious effect.

Reactive Protoplasmic Astrocytes

By dye filling individual astrocytes, Wilhelmsson and others (2006) visualized the entire morphology of reactive protoplasmic astrocytes following two types of injury: deafferentation of the dentate gyrus, and an electrical-induced lesion of the cerebral cortex. The former induces reactivity of astrocytes that is not directly affected by the trauma, whereas in the cortical lesion, reactive astrocytes 200 to 800 μm from the injury border were examined. Four days after these lesions, astrocytes showed hypertrophy of the cell body and processes and an increase in both the number of primary processes leaving the soma (hippocampus, 6.1 v. 5.2; cortex, 6.2 v. 5.1) as well as the number of main processes visible 15 to 25 μm from the soma (hippocampus, 3.1 v. 2.1; cortex, 6.6 v. 3.4). These changes increase the density of processes filling the volume of neuropil occupied by the astrocyte (Fig. 4C and 4D). In other words, these astrocytes become bushier. How long these changes persist or whether they are permanent are unknown.

In contrast, a global ischemic/hypoxic insult induces a different morphological change in cortical astrocytes. Sullivan and others (2010) tracked the remodeling that occurs with increasing insult in the pig cortex. In mild cases, the primary processes become shorter and thicker while maintaining its fine branching pattern (Fig. 4E). As the insult increases, there

is a reduction in the complexity of the branchings, the processes become shorter and thicker and begin to develop bulb-like swellings along their length and at the terminals. In severely damaged cortex, the processes of astrocytes become dramatically reduced in length (Fig. 4E). These changes were observed at 8 and 72 hours postinsult.

The complete morphology of cortical astrocytes has also been studied when the extracellular environment is perturbed, such as following various degrees of hypotonic stress, elevations in $[K^+]_o$, dehydration, overhydration, and ischemia/reperfusion. Such perturbations may follow subtle physiological fluctuations or result from pathology. In most of these cases, there is an increase in the total volume of the astrocyte, except for dehydration, which resulted in shrinkage. Interestingly, the astrocyte population could be segregated according to whether they showed a large volume increase (high-response astrocytes) or a small volume increase (low-response astrocytes). Much of this change is largely accounted for by an increase in the volume of processes rather than the cell body. This highlights the importance of visualizing the processes completely and not relying on GFAP labeling. Despite the overall volume increase, the morphology of different compartments within an individual astrocyte changed in complex ways, including swelling, shrinking, and structural rearrangement (Chvatal and others 2007; Benesova and others 2009; Risher and others 2009). Different compartments of an astrocyte may regulate their own volume (Allansson and others 1999). These volume changes were not seen to affect the overall spatial territory of the astrocyte. In most cases, the morphology returned to normal once the stimulus was removed.

The Spatial Domain Organization of Reactive Protoplasmic Astrocytes Following Injury and Disease

Normal protoplasmic astrocytes in the cortex and hippocampus tile in nonoverlapping spatial domains. Following injury, some studies have suggested that they maintain their nonoverlapping organization (Wilhelmsson and others 2006), while others have reported an overlap (Oberheim and others 2009; Sofroniew 2009).

In studying reactivity following deafferentation (a model of indirect trauma) and direct mechanical lesion (astrocytes 200–800 μm from the lesion were examined), Wilhelmsson and others (2006) found that in both instances, reactive astrocytes maintained their nonoverlapping spatial domains. They continue to maintain very little overlap of neighboring processes, and the volume of neuropil they occupy remains the same (Fig. 4F). However, when initially visualized by antibodies against GFAP, these thicker processes appeared longer because they could be followed over a greater distance. Therefore, it was thought that the size of the astrocyte domain enlarged. In fact, the hypertrophy of the processes does not affect the volume of the domain because the growth occurs within the confines of a domain.

In contrast, studies from the Sofroniew laboratory, which also used models of mechanical trauma, show that protoplasmic astrocytes immediately adjacent to the lesion (<100 μm) have processes that overlap extensively and interdigitate, forming a distinct boundary around the lesion (Bush and others 1999; Sofroniew 2009) (Fig. 4G). This difference may be due to the distance of the astrocytes examined from the lesion core (see section “The Morphological Appearance of the Glial Scar: Are the Changes Reversible?”).

A nonoverlapping domain organization is also preserved in a mouse model of Alzheimer disease but not in epilepsy. One week after an intracortical injection of ferrous chloride to simulate epilepsy, astrocytes directly adjacent to the area of injection (<200 μm), and those further from the injury epicenter (200–1000 μm), show a loss of their domain organization. There was a chronic increase in the volume of neuropil occupied by the astrocyte and a 8- to

15-fold increase in the overlap of neighboring processes (Castiglioni and others 1990; Oberheim and others 2008). Supression of the epileptic seizures using an antiepileptic drug can reduce the morphological changes of individual astrocytes and restore the nonoverlapping domain organization.

Reactive Fibrous Astrocytes

Detailed studies on the morphological changes of reactive fibrous astrocytes have been best performed in the optic nerves of rodents. A significant finding is that reactive fibrous astrocytes remodel very differently to protoplasmic astrocytes following a mechanical injury. In a transection of the optic nerve of immature rats, Butt and Colquhoun (1996) found that hypertrophy of the cell body and processes was the major response to enucleation. However, unlike protoplasmic astrocytes, astrocytes in the myelinated optic nerve showed a reduction in the number of processes and branchings, a thickening of remaining processes, and a withdrawal of radial processes ending at the glia limitans (Fig. 4H and 4I). These changes reduce the overall complexity of the branching structure.

There is a similiar pattern of remodeling following an optic nerve crush (Sun and others 2010). Three days post-crush, reactive astrocytes at the unmyelinated nerve head demonstrate striking morphological changes. There was hypertrophy of the cell bodies and processes, retraction of primary processes (a reduction in the number of processes and branching), and a loss of their transverse orientation (Fig. 5A–E′). Many fine processes, especially those that emanate directly from the soma, were lost. Quantitatively, the processes of these astrocytes thickened nearly two-fold and the number of primary processes leaving the soma halved. Due to the retraction of the processes, the spatial coverage of an individual reactive astrocyte diminished almost eight-fold to approximately 5% of the total surface area of the optic nerve head (Fig. 5C). This pattern of change was similiarly observed for reactive astrocytes in the myelinated optic nerve (Fig. 5F and 5H) and in a white matter region of the brain, the corpus callosum (Sun and others 2010) (Fig. 5G and 5I). Normal fibrous astrocytes overlap extensively in their spatial domain and continue to do so when reactive.

These results demonstrate that fibrous astrocytes react differently from protoplasmic astrocytes following mechanical injury. Fibrous astrocytes retract and simplify their processes, whereas protoplasmic astrocytes increase the number of processes and branches, giving an overall bushier appearance (Fig. 6). The main common feature is the hypertrophy of the cell bodies and processes.

Are Changes in the Morphology of Individual Astrocytes Reversible? Fibrous Astrocytes Show a Two-Stage Remodeling Process

Whether astrocytes revert back to their normal morphology and organization following insult and how long they may take to do so are unclear. Moreover, the extent to which various molecular changes resolve or persist is not well known. Sofroniew (2009) suggests that mild and moderate forms of reactive astrogliosis have the potential for resolution if the triggering mechanism has resolved. Where there is extreme activation of astrocytes in response to overt tissue damage and inflammation, reactive astrocytes form a scar; the morphological changes are long lasting and may persist long after the triggering insult is removed. In general, few studies have assessed the recovery of the astrocyte morphology and organization in the long term (e.g., >2 months).

Myer and others (2006) demonstrated that an up-regulation in the expression of GFAP and hypertrophy can persist up to 28 days after a moderate cortical injury. Interestingly, there was preservation of NeuN-positive neurons and the surrounding cytoarchitecture. In an animal model of epilepsy, administration of the antiepileptic drug valproate reversed the

morphological changes of individual astrocytes and the overlap of processes between adjacent reactive astrocytes (Oberheim and others 2008). A recovery in the morphology of astrocytes has also been observed 2 weeks after an optic nerve crush. The length of the processes increased compared to earlier time points after the crush, the hypertrophy of the processes was reduced, and the number of primary processes leaving the soma increased (compare Fig. 5D–5E′ with Fig. 7A–7B′). This recovery continues for at least 1 month after crush.

This overall pattern of process retraction and thickening followed by re-extension was also observed for fibrous astrocytes in the myelinated portion of the optic nerve and the corpus callosum following injury (Sun and others 2010). Butt and Colquhoun (1996) reported a similiar remodeling process following an optic nerve transection in the rat. Individual fibrous astrocytes therefore undergo a two-stage remodeling process (Fig. 7C). It is unknown why fibrous astrocytes would react in such a way. The shortening of processes would be expected to cause a loss of gap junctional coupling, a detachment of their endfeet from the pial wall and blood vessels, and of processes that might be associated with surviving axons.

The Morphological Appearance of the Glial Scar: Are the Changes Reversible?

The appearance and phases of the glial scar are best studied in models of spinal cord injury, penetrating brain injury and optic nerve crush. These have thus been adopted as the prototypical penetrating injury for documenting scarring in the CNS. Based upon GFAP labeling, characteristic reactive changes in astrocytes surrounding a penetrating lesion occur by 3 to 7 days postinjury. These astrocytes continually repair and contract the lesion area until 2 weeks postinjury, at which time a glial scar is formed (Logan and Berry 2002; Okada and others 2006; Herrmann and others 2008). In models of spinal cord injury, functional recovery parallels the structural remodeling, in that there is continual motor improvement up until 2 weeks when the glial scar forms and improvement plateaus (Okada and others 2006). Loss-of-function studies have characterized the reactive response as having two phases: the first 2 weeks postinjury represents a subacute phase, a time when reactive astrocytes repair tissue and restore function (Sofroniew and Vinters 2010), whereas in the chronic phase of injury (>2 weeks), reactive astrocytes impair axonal regeneration by forming a physical and chemical barrier (Okada and others 2006).

How does a population of reactive astrocytes remodel to form the glial scar? An important characteristic of scar formation is that astrocytes directly adjacent to the lesion site respond differently from those at more distant locations (Fig. 7D and 7E). Oberheim and others (2009) demonstrated two morphologically distinct types of reactive astrocytes forming the glial scar and surrounding the injury site. Astrocytes directly adjacent to the area of injection (<200 μm) have processes arranged in a radial pattern around the core, effectively forming a physical barrier separating the lesion from the surrounding cortical tissue. These “palisading” astrocytes have processes that are mainly straight and lack the profuse and delicate ramifications of normal protoplasmic astrocytes in the cortex (Fig. 7E). The processes of neighboring palisading astrocytes overlap extensively, and thus, the astrocytes exhibit a loss of individual domains. Astrocytes further from the injury epicenter (200–1000 μm) were termed hypertrophic (Fig. 7E). These astrocytes demonstrate less pronounced changes in their morphology, appearing somewhat similar to normal protoplasmic astrocytes. When subjected to quantitative analysis, however, hypertrophic astrocytes showed thickening of processes and an overlap in their domains.

Work from the Sofroniew laboratory has also described this spatially distinct response after traumatic injury and inflammation in both gray (cortex/hippocampus) (Fig. 7F) and white matter (spinal cord) (Fig. 7G). Reactive astrocytes within the lesion boundary zone (also found to be <200 μm) are densely packed and closely abutting with tightly interdigitating processes that form a continuous unbroken boundary around the core of the lesion (Herrmann and others 2008, 2010; Sofroniew 2009) (Figs. 4G, 7F, and 7G).

In summary, the loss of the discrete domains appears to be a characteristic of severe reactive astrogliosis in the gray matter and generally occurs at the border (<200 μm) of a persistent mature glial scar. Moving away from the epicenter of the lesion, astrocytes show less pronounced reactive changes. Normal fibrous astrocytes of the white matter overlap in their spatial domains and continue to do so when they form a glial scar.

The appearance of the glial scar has been well documented using GFAP labeling, but what a glial scar actually looks like remains unclear. Visualizing EGFP-expressing reactive astrocytes in the crushed optic nerve reveals a dramatic reorganization of the normal astrocytic architecture (Sun and others 2010). This is particularly apparent in the optic nerve head because in normal animals, there is a distinct arrangement of the astrocytes (Sun and others 2009).

The processes of astrocytes in the normal optic nerve head form glial tubes through which the ganglion cell axons travel, giving the glial architecture within this region a honeycomb appearance. This can be seen upon labeling with GFAP (Fig. 1B) and in the hGFAPpr-EGFP transgenic animal (Howell and others 2007; Sun and others 2009) (Fig. 5B). These astrocytes also arrange themselves to form sheets aligned transversely across the nerve (Fig. 5A). Three days postcrush, there is a dramatic remodeling of the glial architecture, consisting of a loss of the glial tubes and the overall honeycomb appearance (Fig. 5D–Fig. 5E′). Many astrocytes lose their transverse orientation (Fig. 5D). The individual astrocytes appear bulbous in shape, and there now exists a dense meshwork of disorganized processes (Fig. 5E). Astrocytes fill in all the space within the optic nerve head. This spatial disorganization persists through to 7 days postcrush. By 2 weeks, there is recovery in the overall architecture of this region, and a dense glial scar is formed. There is partial re-extension of the astrocyte processes, and they are thinner. However, there is no recovery of the glial tube or honeycomb arrangement (Fig. 7B).

What is the purpose of the glial scar? From a purely anatomical standpoint, the glial scar may provide beneficial structural support. In cases where there is a partial lesion, the scar may fill in the space devoid of axons and function as a scaffold, preventing the tissue from shrinking and causing damage to the surviving axons. On the other hand, the classic detrimental effect of the glial scar is the inhibition of axon regeneration. Traditionally thought to simply be a mechanical barrier, later studies demonstrated that the molecular composition of the scar and the production of inhibitory molecules by reactive astrocytes are contributing factors for regenerative failure (Yiu and He 2006; Fitch and Silver 2008; Sofroniew 2009). In this example of the optic nerve head, once a scar is formed within this region, it is difficult to see how, if axons were to regenerate, they would reorganize to form bundles with a topographic relationship to the retina. It may be that the presence of axons is required for the astrocytes to arrange themselves in glial tubes and hence form the honeycomb-like structure.

Conclusion and Future Directions

Astrocytes are a diverse population of cells, differing across the CNS in their morphology, physiology, and function. Their importance is being discovered in protoplasmic and fibrous astrocytes, and future work will need to determine whether all astrocytes share the same

characteristics. Visualizing the complete morphology of normal and reactive astrocytes has revealed their domain organization, demonstrated that not all astrocytes remodel in the same way, and shown the plasticity of remodeling (e.g., the two-stage remodeling of fibrous astrocytes). Revealing their structure has allowed a better understanding of how they interact with the surrounding neural elements.

But many questions remain. What is the functional purpose of remodeling? How long do the reactive morphological changes last, and do astrocytes regain their organization (e.g., reform the honeycomb arrangement in the optic nerve head, reconnect with blood vessels, form new gap junctions). What do astrocytes in a very old glial scar look like? For example, one that is 6 months old, or even several years, such as in patients with an old gliosis. If astrocytes continue to show an increased expression of GFAP in the long term (e.g., >6–12 months), should they still be considered “reactive,” or have they achieved a new steady state? Myer and others (2006) showed that astrocytes can maintain high levels of GFAP for as long as 28 days postinjury while the surrounding neuronal cytoarchitecture is still preserved. Studies using cell type–specific gene deletion in transgenic animals that have GFP-expressing astrocytes may provide an approach to dissecting the molecular pathways involved in the reactive structural changes.

Acknowledgments

Funding

The author(s) disclosed receipt of the following financial support for the research and/or authorship of this article: This work was supported by National Institutes of Health (NIH) grants RO1 017169 and RO1 EY019703 and grants from The Glaucoma Foundation, The American Health Assistance Foundation (AHAF), and Research to Prevent Blindness (RPB).

References

Allansson L, Khatibi S, Gustavsson T, Blomstrand F, Olsson T, Hansson E. Single-cell volume estimation by three-dimensional wide-field microscopy applied to astroglial primary cultures. J Neurosci Methods. 1999; 93(1):1–11. [PubMed: 10598859]

Angulo MC, Kozlov AS, Charpak S, Audinat E. Glutamate released from glial cells synchronizes neuronal activity in the hippocampus. J Neurosci. 2004; 24(31):6920–7. [PubMed: 15295027]

Bachoo RM, Kim RS, Ligon KL, Maher EA, Brennan C, Billings N, et al. Molecular diversity of astrocytes with implications for neurological disorders. Proc Natl Acad Sci U S A. 2004; 101(22): 8384–9. [PubMed: 15155908]

Benediktsson AM, Schachtele SJ, Green SH, Dailey ME. Ballistic labeling and dynamic imaging of astrocytes in organotypic hippocampal slice cultures. J Neurosci Methods. 2005; 141(1):41–53. [PubMed: 15585287]

Benesova J, Hock M, Butenko O, Prajerova I, Anderova M, Chvatal A. Quantification of astrocyte volume changes during ischemia in situ reveals two populations of astrocytes in the cortex of GFAP/EGFP mice. J Neurosci Res. 2009; 87(1):96–111. [PubMed: 18752295]

Bezzi P, Gundersen V, Galbete JL, Seifert G, Steinhäuser C, Pilati E, et al. Astrocytes contain a vesicular compartment that is competent for regulated exocytosis of glutamate. Nat Neurosci. 2004; 7(6):613–20. [PubMed: 15156145]

Blomstrand F, Aberg ND, Eriksson PS, Hansson E, Rönnbäck L. Extent of intercellular calcium wave propagation is related to gap junction permeability and level of connexin-43 expression in astrocytes in primary cultures from four brain regions. Neuroscience. 1999; 92(1):255–65. [PubMed: 10392848]

Buffo A, Rolando C, Ceruti S. Astrocytes in the damaged brain: molecular and cellular insights into their reactive response and healing potential. Biochem Pharmacol. 2010; 79(2):77–89. [PubMed: 19765548]

Bush TG, Puvanachandra N, Horner CH, Polito A, Ostenfeld T, Svendsen CN, et al. Leukocyte infiltration, neuronal degeneration, and neurite outgrowth after ablation of scar-forming, reactive astrocytes in adult transgenic mice. Neuron. 1999; 23(2):297–308. [PubMed: 10399936]

Bushong EA, Martone ME, Jones YZ, Ellisman MH. Protoplasmic astrocytes in CA1 stratum radiatum occupy separate anatomical domains. J Neurosci. 2002; 22(1):183–92. [PubMed: 11756501]

Butt A, Colquhoun K. Glial cells in transected optic nerves of immature rats: I. An analysis of individual cells by intracellular dye-injection. J Neurocytol. 1996; 25(6):365–80. [PubMed: 8835785]

Butt A, Colquhoun K, Berry M. Confocal imaging of glial cells in the intact rat optic nerve. Glia. 1994a; 10(4):315–22. [PubMed: 7520025]

Butt A, Colquhoun K, Tutton M, Berry M. Three-dimensional morphology of astrocytes and oligodendrocytes in the intact mouse optic nerve. J Neurocytol. 1994b; 23(8):469–85. [PubMed: 7527074]

Butt A, Duncan A, Berry M. Astrocyte associations with nodes of Ranvier: ultrastructural analysis of HRP-filled astrocytes in the mouse optic nerve. J Neurocytol. 1994c; 23(8):486–99. [PubMed: 7983475]

Cahoy JD, Emery B, Kaushal A, Foo LC, Zamanian JL, Christopherson KS, et al. A transcriptome database for astrocytes, neurons, and oligodendrocytes: a new resource for understanding brain development and function. J Neurosci. 2008; 28(1):264–78. [PubMed: 18171944]

Castiglioni AJ, Peterson SL, Sanabria EL, Tiffany-Castiglioni E. Structural changes in astrocytes induced by seizures in a mode of temporal lobe epilepsy. J Neurosci Res. 1990; 26(3):334–41. [PubMed: 2398512]

Chan-Ling T, Stone J. Factors determining the morphology and distribution of astrocytes in the cat retina: a ‘contact-spacing’ model of astrocyte interaction. J Comp Neurol. 1991; 303(3):375–86. [PubMed: 2007655]

Chaudhry FA, Lehre KP, van Lookeren Campagne M, Ottersen OP, Danbolt NC, Storm-Mathisen J. Glutamate transporters in glial plasma membranes: highly differentiated localizations revealed by quantitative ultrastructural immunocytochemistry. Neuron. 1995; 15(3):711–20. [PubMed: 7546749]

Chvátal A, Anderová M, Hock M, Prajerová I, Neprasová H, Chvátal V, et al. Three-dimensional confocal morphometry reveals structural changes in astrocyte morphology in situ. J Neurosci Res. 2007; 85(2):260–71. [PubMed: 17086549]

Chvátal A, Pastor A, Mauch M, Sykova E, Kettenmann H. Distinct populations of identified glial cells in the developing rat spinal cord slice: ion channel properties and cell morphology. Eur J Neurosci. 1995; 7(1):129–42. [PubMed: 7536092]

Connor JR, Berkowitz EM. A demonstration of glial filament distribution in astrocytes isolated from rat cerebral cortex. Neuroscience. 1985; 16(1):33–44. [PubMed: 2423916]

Cornell-Bell A, Thomas P, Smith S. The excitatory neurotransmitter glutamate causes filopodia formation in cultured hippocampal astrocytes. Glia. 1990; 3(5):322–34. [PubMed: 1699891]

D’Ambrosio R, Wenzel J, Schwartzkroin PA, McKhann GM, Janigro D. Functional specialization and topographic segregation of hippocampal astrocytes. J Neurosci. 1998; 18(12):4425–38. [PubMed: 9614220]

Deloulme JC, Raponi E, Gentil BJ, Bertacchi N, Marks A, Labourdette G, et al. Nuclear expression of S100B in oligodendrocyte progenitor cells correlates with differentiation toward the oligodendroglial lineage and modulates oligodendrocytes maturation. Mol Cell Neurosci. 2004; 27(4):453–65. [PubMed: 15555923]

Denis-Donini S, Glowinski J, Prochiantz A. Glial heterogeneity may define the three-dimensional shape of mouse mesencephalic dopaminergic neurones. Nature. 1984; 307(5952):641–3. [PubMed: 6694754]

Doyle JP, Dougherty JD, Heiman M, Schmidt EF, Stevens TR, Ma G, et al. Application of a translational profiling approach for the comparative analysis of CNS cell types. Cell. 2008; 135(4): 749–62. [PubMed: 19013282]

Drejer J, Larsson O, Schousboe A. Characterization of L-glutamate uptake into and release from astrocytes and neurons cultured from different brain regions. Exp Brain Res. 1982; 47(2):259–69. [PubMed: 6126390]

Emsley JG, Macklis JD. Astroglial heterogeneity closely reflects the neuronal-defined anatomy of the adult murine CNS. Neuron Glia Biol. 2006; 2(3):175–86. [PubMed: 17356684]

Eng L, Gerstl B, Vanderhaegen JJ. A study of proteins in old multiple sclerosis plaques. Trans Am Soc Neurochem. 1970; 1:42.

Eng L, Ghirnikar R, Lee Y. Glial fibrillary acidic protein: GFAP-thirty-one years (1969–2000). Neurochem Res. 2000; 25(9–10):1439–51. [PubMed: 11059815]

Fellin T, Pascual O, Gobbo S, Pozzan T, Haydon PG, Carmignoto G. Neuronal synchrony mediated by astrocytic glutamate through activation of extrasynaptic NMDA receptors. Neuron. 2004; 43(5): 729–43. [PubMed: 15339653]

Fitch MT, Silver J. CNS injury, glial scars, and inflammation: inhibitory extracellular matrices and regeneration failure. Exp Neurol. 2008; 209(2):294–301. [PubMed: 17617407]

Gan WB, Grutzendler J, Wong WT, Wong RO, Lichtman JW. Multicolor “DiOlistic” labeling of the nervous system using lipophilic dye combinations. Neuron. 2000; 27(2):219–25. [PubMed: 10985343]

Garcia-Abreu J, Neto V, Carvalho S, Cavalcante L. Regionally specific properties of midbrain glia: I. Interactions with midbrain neurons. J Neurosci Res. 1995; 40(4):471–7. [PubMed: 7616607]

Garcia-Segura L, Luqín S, Parducz A, Naftolin F. Gonadal hormone regulation of glial fibrillary acidic protein immunoreactivity and glial ultrastructure in the rat neuroendocrine hypothalamus. Glia. 1994; 10(1):59–69. [PubMed: 8300192]

Genoud C, Quairiaux C, Steiner P, Hirling H, Welker E, Knott GW. Plasticity of astrocytic coverage and glutamate transporter expression in adult mouse cortex. PLoS Biol. 2006; 4(11):e343. [PubMed: 17048987]

Gonçalves C-A, Leite MC, Nardin P. Biological and methodological features of the measurement of S100B, a putative marker of brain injury. Clin Biochem. 2008; 41(10–11):755–63. [PubMed: 18454941]

Gourine AV, Kasymov V, Marina N, Tang F, Figueiredo MF, Lane S, et al. Astrocytes control breathing through pH-dependent release of ATP. Science. 2010; 329(5991):571–5. [PubMed: 20647426]

Haber M, Zhou L, Murai KK. Cooperative astrocyte and dendritic spine dynamics at hippocampal excitatory synapses. J Neurosci. 2006; 26(35):8881–91. [PubMed: 16943543]

Hachem S, Aguirre A, Vives V, Marks A, Gallo V, Legraverend C. Spatial and temporal expression of S100B in cells of oligodendrocyte lineage. Glia. 2005; 51(2):81–97. [PubMed: 15782413]

Halassa MM, Fellin T, Takano H, Dong J-H, Haydon PG. Synaptic islands defined by the territory of a single astrocyte. J Neurosci. 2007; 27(24):6473–7. [PubMed: 17567808]

Hatten ME. Neuronal regulation of astroglial morphology and proliferation in vitro. J Cell Biol. 1985; 100(2):384–96. [PubMed: 3881455]

Heintz N. Gene expression nervous system atlas (GEN-SAT). Nat Neurosci. 2004; 7(5):483. [PubMed: 15114362]

Herrmann JE, Imura T, Song B, Qi J, Ao Y, Nguyen TK, et al. STAT3 is a critical regulator of astrogliosis and scar formation after spinal cord injury. J Neurosci. 2008; 28(28):7231–43. [PubMed: 18614693]

Herrmann JE, Shah RR, Chan AF, Zheng B. EphA4 deficient mice maintain astroglial-fibrotic scar formation after spinal cord injury. Exp Neurol. 2010; 223(2):582–98. [PubMed: 20170651]

Hirrlinger J, Hülsmann S, Kirchhoff F. Astroglial processes show spontaneous motility at active synaptic terminals in situ. Eur J Neurosci. 2004; 20(8):2235–9. [PubMed: 15450103]

Houades V, Koulakoff A, Ezan P, Seif I, Giaume C. Gap junction-mediated astrocytic networks in the mouse barrel cortex. J Neurosci. 2008; 28(20):5207–17. [PubMed: 18480277]

Howell GR, Libby RT, Jakobs TC, Smith RS, Phalan FC, Barter JW, et al. Axons of retinal ganglion cells are insulted in the optic nerve early in DBA/2J glaucoma. J Cell Biol. 2007; 179(7):1523–37. [PubMed: 18158332]

Huang YH, Bergles DE. Glutamate transporters bring competition to the synapse. Curr Opin Neurobiol. 2004; 14(3):346–52. [PubMed: 15194115]

Iadecola C, Nedergaard M. Glial regulation of the cerebral microvasculature. Nat Neurosci. 2007; 10(11):1369–76. [PubMed: 17965657]

Israel J-M, Schipke CG, Ohlemeyer C, Theodosis DT, Kettenmann H. GABAA receptor-expressing astrocytes in the supraoptic nucleus lack glutamate uptake and receptor currents. Glia. 2003; 44(2): 102–10. [PubMed: 14515326]

Jabs R, Paterson IA, Walz W. Qualitative analysis of membrane currents in glial cells from normal and gliotic tissue in situ: down-regulation of Na+ current and lack of P2 purinergic responses. Neuroscience. 1997; 81(3):847–60. [PubMed: 9316033]

Jones TA, Greenough WT. Ultrastructural evidence for increased contact between astrocytes and synapses in rats reared in a complex environment. Neurobiol Learn Mem. 1996; 65(1):48–56. [PubMed: 8673406]

Kang W, Hébert JM. Signaling pathways in reactive astrocytes, a genetic perspective. Mol Neurobiol. 2011; 43(3):147–54. [PubMed: 21234816]

Káradóttir R, Hamilton NB, Bakiri Y, Attwell D. Spiking and nonspiking classes of oligodendrocyte precursor glia in CNS white matter. Nat Neurosci. 2008; 11(4):450–6. [PubMed: 18311136]

Klintsova A, Levy WB, Desmond NL. Astrocytic volume fluctuates in the hippocampal CA1 region across the estrous cycle. Brain Res. 1995; 690(2):269–74. [PubMed: 8535849]

Kosaka T, Hama K. Three-dimensional structure of astrocytes in the rat dentate gyrus. J Comp Neurol. 1986; 249(2):242–60. [PubMed: 3525618]

Kozlov AS, Angulo MC, Audinat E, Charpak S. Target cell-specific modulation of neuronal activity by astrocytes. Proc Natl Acad Sci U S A. 2006; 103(26):10058–63. [PubMed: 16782808]

Kullmann DM, Asztely F. Extrasynaptic glutamate spill-over in the hippocampus: evidence and implications. Trends Neurosci. 1998; 21(1):8–14. [PubMed: 9464678]

Lee S, Kim W, Cornell-Bell A, Sontheimer H. Astrocytes exhibit regional specificity in gap-junction coupling. Glia. 1994; 11(4):315–25. [PubMed: 7960035]

Lehre KP, Levy LM, Ottersen OP, Storm-Mathisen J, Danbolt NC. Differential expression of two glial glutamate transporters in the rat brain: quantitative and immunocytochemical observations. J Neurosci. 1995; 15(3 Pt 1):1835–53. [PubMed: 7891138]

Livet J, Weissman TA, Kang H, Draft RW, Lu J, Bennis RA, et al. Transgenic strategies for combinatorial expression of fluorescent proteins in the nervous system. Nature. 2007; 450(7166): 56–62. [PubMed: 17972876]

Lo DC, McAllister AK, Katz LC. Neuronal transfection in brain slices using particle-mediated gene transfer. Neuron. 1994; 13(6):1263–8. [PubMed: 7993619]

Logan, A.; Berry, M. Cellular and molecular determinants of glial scar formation. In: Alzheimer, C., editor. Molecular and cellular biology of neuroprotection in the CNS. New York: Kluwer Academic/Plenum Publishers; 2002. p. 115-58.

Lovatt D, Sonnewald U, Waagepetersen HS, Schousboe A, He W, Lin JH-C, et al. The transcriptome and metabolic gene signature of protoplasmic astrocytes in the adult murine cortex. J Neurosci. 2007; 27(45):12255–66. [PubMed: 17989291]

Lushnikova I, Skibo G, Muller D, Nikonenko I. Synaptic potentiation induces increased glial coverage of excitatory synapses in CA1 hippocampus. Hippocampus. 2009; 19(8):753–62. [PubMed: 19156853]

Maxwell D, Kruger L. The fine structure of astrocytes in the cerebral cortex and their response to focal injury produced by heavy ionizing particles. J Cell Biol. 1965; 25(2):141–57. [PubMed: 19866658]

Middeldorp J, Hol EM. GFAP in health and disease. Prog Neurobiol. 2011; 93(3):421–43. [PubMed: 21219963]

Mothet J-P, Pollegioni L, Ouanounou G, Martineau M, Fossier P, Baux G. Glutamate receptor activation triggers a calcium-dependent and SNARE protein-dependent release of the gliotransmitter D-serine. Proc Natl Acad Sci U S A. 2005; 102(15):5606–11. [PubMed: 15800046]

Müller T, Möller T, Berger T, Schnitzer J, Kettenmann H. Calcium entry through kainite receptors and resulting posassium-channel blockade in Bergmann glial cells. Science. 1992; 256(5063):1563–6. [PubMed: 1317969]

Murai KK, Nguyen LN, Irie F, Yamaguchi Y, Pasquale EB. Control of hippocampal dendritic spine morphology through ephrin-A3/EphA4 signaling. Nat Neurosci. 2003; 6(2):153–60. [PubMed: 12496762]

Myer DJ, Gurkoff GG, Lee SM, Hovda DA, Sofroniew MV. Essential protective roles of reactive astrocytes in traumatic brain injury. Brain. 2006; 129(Pt 10):2761–72. [PubMed: 16825202]

Nolte C, Matyash M, Pivneva T, Schipke CG, Ohlemeyer C, Hanisch UK, et al. GFAP promoter-controlled EGFP-expressing transgenic mice: a tool to visualize astrocytes and astrogliosis in living brain tissue. Glia. 2001; 33(1):72–86. [PubMed: 11169793]

Oberheim NA, Takano T, Han X, He W, Lin JHC, Wang F, et al. Uniquely hominid features of adult human astrocytes. J Neurosci. 2009; 29(10):3276–87. [PubMed: 19279265]

Oberheim NA, Tian G-F, Han X, Peng W, Takano T, Ransom B, et al. Loss of astrocytic domain organization in the epileptic brain. J Neurosci. 2008; 28(13):3264–76. [PubMed: 18367594]

Oberheim NA, Wang X, Goldman S, Nedergaard M. Astrocytic complexity distinguishes the human brain. Trends Neurosci. 2006; 29(10):547–53. [PubMed: 16938356]

Ogata K, Kosaka T. Structural and quantitative analysis of astrocytes in the mouse hippocampus. Neuroscience. 2002; 113(1):221–33. [PubMed: 12123700]

Okada S, Nakamura M, Katoh H, Miyao T, Shimazaki T, Ishii K, et al. Conditional ablation of Stat3 or Socs3 discloses a dual role for reactive astrocytes after spinal cord injury. Nat Med. 2006; 12(7): 829–34. [PubMed: 16783372]

Panatier A, Oliet S. Neuron-glia interactions in the hypothalamus. Neuron Glia Biol. 2006; 2(1):51–8. [PubMed: 18634590]

Parpura, V.; Haydon, P., editors. Astrocytes in (patho)physiology of the nervous system. New York: Springer; 2009.

Pascual O, Casper K, Kubera C, Zhang J, Revilla-Sanchez R, Sul JY, et al. Astrocytic purinergic signaling coordinates synaptic networks. Science. 2005; 310(5745):113–6. [PubMed: 16210541]

Pastor A, Chvatal A, Sykova E, Kettenmann H. Glycine- and GABA-activated currents in identified glial cells of the developing rat spinal cord slice. Eur J Neurosci. 1995; 7(6):1188–98. [PubMed: 7582092]

Pekny M, Johansson CB, Eliasson C, Stakeberg J, Wallén A, Perlmann T, et al. Abnormal reaction to central nervous system injury in mice lacking glial fibrillary acidic protein and vimentin. J Cell Biol. 1999; 145(3):503–14. [PubMed: 10225952]

Pekny M, Nilsson M. Astrocyte activation and reactive gliosis. Glia. 2005; 50(4):427–34. [PubMed: 15846805]

Pellerin L, Bouzier-Sore A-K, Aubert A, Serres S, Merle M, Costalat R, et al. Activity-dependent regulation of energy metabolism by astrocytes: an update. Glia. 2007; 55(12):1251–62. [PubMed: 17659524]

Raine C. On the association between perinodal astrocytic processes and the node of Ranvier in the CNS. J Neurocytol. 1984; 13(1):21–7. [PubMed: 6707711]

Regan MR, Huang YH, Kim YS, Dykes-Hoberg MI, Jin L, Watkins AM, et al. Variations in promoter activity reveal a differential expression and physiology of glutamate transporters by glia in the developing and mature CNS. J Neurosci. 2007; 27(25):6607–19. [PubMed: 17581948]

Reichenbach, A.; Wolburg, H. Astrocytes and ependymal glia. In: Parpura, A.; Haydon, P., editors. Astrocytes in (patho)physiology of the nervous system. New York: Springer; 2009. p. 19-33.

Ridet J, Privat A, Malhotra S, Gage F. Reactive astrocytes: cellular and molecular cues to biological function. Trends Neurosci. 1997; 20(12):570–7. [PubMed: 9416670]

Risher WC, Andrew RD, Kirov SA. Real-time passive volume responses of astrocytes to acute osmotic and ischemic stress in cortical slices and in vivo revealed by two-photon microscopy. Glia. 2009; 57(2):207–21. [PubMed: 18720409]

Robel S, Berninger B, Götz M. The stem cell potential of glia: lessons from reactive gliosis. Nat Rev Neurosci. 2011; 12(2):88–104. [PubMed: 21248788]

Rodríguez JJ, Olabarria M, Chvatal A, Verkhratsky A. Astroglia in dementia and Alzheimer's disease. Cell Death Differ. 2009; 16(3):378–85. [PubMed: 19057621]

Rouach N, Koulakoff A, Abudara V, Willecke K, Giaume C. Astroglial metabolic networks sustain hippocampal synaptic transmission. Science. 2008; 322(5907):1551–5. [PubMed: 19056987]

Schmitt A, Asan E, Püschel B, Kugler P. Cellular and regional distribution of the glutamate transporter GLAST in the CNS of rats: nonradioactive in situ hybridization and comparative immunocytochemistry. J Neurosci. 1997; 17(1):1–10. [PubMed: 8987731]

Simard M, Nedergaard M. The neurobiology of glia in the context of water and ion homeostasis. Neuroscience. 2004; 129(4):877–96. [PubMed: 15561405]

Sobue G, Pleasure D. Astroglial proliferation and phenotype are modulated by neuronal plasma membrane. Brain Res. 1984; 324(1):175–9. [PubMed: 6518388]

Soffié M, Hahn K, Terao E, Eclancher F. Behavioural and glial changes in old rats following environmental enrichment. Behav Brain Res. 1999; 101(1):37–49. [PubMed: 10342398]

Sofroniew M. Molecular dissection of reactive astrogliosis and glial scar formation. Trends Neurosci. 2009; 32(12):638–47. [PubMed: 19782411]

Sofroniew MV, Vinters HV. Astrocytes: biology and pathology. Acta Neuropathol. 2010; 119(1):7–35. [PubMed: 20012068]

Steiner J, Bernstein H-G, Bielau H, Berndt A, Brisch R, Mawrin C, et al. Evidence for a wide extra-astrocytic distribution of S100B in human brain. BMC Neurosci. 2007; 8:2. [PubMed: 17199889]

Steinhaüser C, Berger T, Frotscher M, Kettenmann H. Heterogeneity in the membrane current pattern of identified glial cells in the hippocampal slice. Eur J Neurosci. 1992; 4(6):472–84. [PubMed: 12106333]

Sul JY, Orosz G, Givens RS, Haydon P. Astrocytic connectivity in the hippocampus. Neuron Glia Biol. 2004; 1(1):3–11. [PubMed: 16575432]

Sullivan SM, Björkman ST, Miller SM, Colditz PB, Pow DV. Structural remodeling of gray matter astrocytes in the neonatal pig brain after hypoxia/ischemia. Glia. 2010; 58(2):181–94. [PubMed: 19606499]

Sun D, Lye-Barthel M, Masland RH, Jakobs TC. The morphology and spatial arrangement of astrocytes in the optic nerve head of the mouse. J Comp Neurol. 2009; 516(1):1–19. [PubMed: 19562764]

Sun D, Lye-Barthel M, Masland RH, Jakobs TC. Structural remodeling of fibrous astrocytes after axonal injury. J Neurosci. 2010; 30(42):14008–19. [PubMed: 20962222]

Suzuki R, Watanabe J, Arata S, Funahashi H, Kikuyama S, Shioda S. A transgenic mouse model for the detailed morphological study of astrocytes. Neurosci Res. 2003; 47(4):451–4. [PubMed: 14630350]

Sykova E. Extrasynaptic volume transmission and diffusion parameters of the extracellular space. Neuroscience. 2004; 129(4):861–76. [PubMed: 15561404]

Tout S, Dreher Z, Chan-Ling T, Stone J. Contact-spacing among astrocytes is independent of neighbouring structures: in vivo and in vitro evidence. J Comp Neurol. 1993; 332(4):433–43. [PubMed: 8349842]

Ullian E, Sapperstein S, Christopherson K, Barres B. Control of synapse number by glia. Science. 2001; 291(5504):657–61. [PubMed: 11158678]

Ventura R, Harris KM. Three-dimensional relationships between hippocampal synapses and astrocytes. J Neurosci. 1999; 19(16):6897–906. [PubMed: 10436047]

Viola GG, Rodrigues L, Américo JC, Hansel G, Vargas RS, Biasibetti R, et al. Morphological changes in hippocampal astrocytes induced by environmental enrichment in mice. Brain Res. 2009; 1274:47–54. [PubMed: 19374889]

Vives V, Alonso G, Solal AC, Joubert D, Legraverend C. Visualization of S100B-positive neurons and glia in the central nervous system of EGFP transgenic mice. J Comp Neurol. 2003; 457(4):404–19. [PubMed: 12561079]

Wallraff A, Odermatt B, Willecke K, Steinhäuser C. Distinct types of astroglial cells in the hippocampus differ in gap junction coupling. Glia. 2004; 48(1):36–43. [PubMed: 15326613]

Walz W. Controversy surrounding the existence of discrete functional classes of astrocytes in adult gray matter. Glia. 2000; 31(2):95–103. [PubMed: 10878596]

Walz W, Lang MK. Immunocytochemical evidence for a distinct GFAP-negative subpopulation of astrocytes in the adult rat hippocampus. Neurosci Lett. 1998; 257(3):127–30. [PubMed: 9870336]

Waxman SG, Black JA. Freeze-fracture ultrastructure of the perinodal astrocyte and associated glial junctions. Brain Res. 1984; 308(1):77–87. [PubMed: 6434150]

Wilhelmsson U, Bushong EA, Price DL, Smarr BL, Phung V, Terada M, et al. Redefining the concept of reactive astrocytes as cells that remain within their unique domains upon reaction to injury. Proc Natl Acad Sci U S A. 2006; 103(46):17513–8. [PubMed: 17090684]

Wilhelmsson U, Li L, Pekna M, Berthold C-H, Blom S, Eliasson C, et al. Absence of glial fibrillary acidic protein and vimentin prevents hypertrophy of astrocytic processes and improves post-traumatic regeneration. J Neurosci. 2004; 24(21):5016–21. [PubMed: 15163694]

Woolley CS, Gould E, Frankfurt M, McEwen BS. Naturally occurring fluctuation in dendritic spine density on adult hippocampal pyramidal neurons. J Neurosci. 1990; 10(12):4035–9. [PubMed: 2269895]

Yamaguchi M, Saito H, Suzuki M, Mori K. Visualization of neurogenesis in the central nervous system using nestin promoter-GFP transgenic mice. Neuroreport. 2000; 11(9):1991–6. [PubMed: 10884058]

Yeh T, Da Yong Lee S, Gutmann D. Microarray analyses reveal regional astrocyte heterogeneity with implications for neurofibromatosis type 1 (NF1)-regulated glial proliferation. Glia. 2009; 57(11): 1239–49. [PubMed: 19191334]

Yiu G, He Z. Glial inhibition of CNS axon regeneration. Nat Rev Neurosci. 2006; 7(8):617–27. [PubMed: 16858390]

Zhang Q, Pangrsic T, Kreft M, Krzan M, Li N, Sul J-Y, et al. Fusion-related release of glutamate from astrocytes. J Biol Chem. 2004; 279(13):12724–33. [PubMed: 14722063]

Zhou M, Kimelberg HK. Freshly isolated hippocampal CA1 astrocytes comprise two populations differing in glutamate transporter and AMPA receptor expression. J Neurosci. 2001; 21(20): 7901–8. [PubMed: 11588163]

Zhuo L, Sun B, Zhang CL, Fine A, Chiu SY, Messing A. Live astrocytes visualized by green fluorescent protein in transgenic mice. Dev Biol. 1997; 187(1):36–42. [PubMed: 9224672]

Box 1

Methods of Visualizing the Morphology of Astrocytes

Immunohistochemistry

Astrocytes can be immunohistochemically labeled by antibodies against their intermediate filaments or cytoplasmic/membrane-bound proteins. Expression of GFAP has become the prototypical marker for the immunohistochemical identification of astrocytes. GFAP was first isolated in high concentrations from old demyelinated plaques of patients with multiple sclerosis and was then found to be associated immunohistochemically with reactive astrocytes in such plaques and in other pathological contexts (Eng and others 1970, 2000). Because of its initial identification in disease, elevated expression of GFAP is now regarded as a sensitive and reliable marker of reactive astrocytes that are responding to CNS injuries. The classic characteristic of a reactive astrocyte (e.g., thickening of the cell body and processes) was defined by GFAP labeling. Several other antibodies against intermediate filaments are also commonly used to label normal and reactive astrocytes, such as vimentin and nestin.

Antibodies against GFAP label only the main processes of an astrocyte that contain intermediate filaments. Neither the full length of the main processes or the fine processes are revealed (see figure in this Box). In fact, GFAP delineates only approximately 15% of the total volume of an astrocyte, leaving the true morphology of an astrocyte unseen. Consequently, GFAP immunohistochemistry underestimates the branching pattern and territory of an astrocyte in comparison with other means of detection such as Golgi staining, expression of reporter proteins such as GFP, or filling with fluorescent dyes (Maxwell and Kruger 1965; Connor and Berkowitz 1985; Bushong and others 2002).

There are other limitations with the use of GFAP. GFAP is not immunohistochemically detectable in all normal astrocytes, its expression exhibiting both regional and local variability. GFAP has a preference for protoplasmic astrocytes, fibrous astrocytes, Bergmann glia, and subependymal astrocytes adjacent to the cerebral ventricles. For example, GFAP is expressed by virtually all Bergmann glial cells in the cerebellum, whereas only about 15% to 20% of astrocytes express GFAP in the cortex and hippocampus. Moreover, GFAP mRNA is predominantly expressed in white matter (Cahoy and others 2008).

Cytoplasmic or membrane protein markers such as S100 calcium-binding protein β (S100β), glutamine synthetase (GS), or glutamate/aspartate transporter (GLAST) can reveal the fine processes of an astrocyte but may produce a labeling pattern with little separation between neighboring astrocytes. Moreover, some of these markers are not exclusive to astrocytes. Although GLAST is specific for astrocytes (Chaudhry and others 1995; Lehre and others 1995; Schmitt and others 1997), antibodies against S100β also label oligodendrocytes, NG2 glial cells, and even neurons (Vives and others 2003; Deloulme and others 2004; Hachem and others 2005; Steiner and others 2007; Goncalves and others 2008).

A significant problem that remains with the current set of immunohistochemical markers is that there are no reliable markers for different types of astrocytes. Therefore, in many cases, it is unknown whether the behavior of an astrocyte is a general property of all astrocytes or of a particular type. Perhaps an analysis on the transcriptome of astrocytes from different brain regions will reveal more selective molecular markers.

Single Cell Dye Injections

Fluorescent indicators can be loaded into individual astrocytes using sharp microelectrodes or patch pipettes. Because of the small diameter of sharp electrodes, iontophoresis, the ejection of a substance by the application of current, is required. Single cell dye injection approaches are technically demanding and time consuming, and only a small number of astrocytes can be labeled at any one time. The primary advantage is that the entire morphology of the astrocyte can be visualized, even the finest of processes. Either live or lightly fixed tissue can be used for these experiments. Compounds used to load the astrocytes either fill the cytoplasm or stain the lipophilic plasma membrane; these include lucifer yellow, carbocyanine dyes such as DiI or DiO, biocytin, neurobiotin and dextran-coupled fluororescein, or rhodamine isothiocyanate. Using various combinations of dyes, neighboring astrocytes can be labeled in different colors.

Particle-Mediated Dye Transfer

Populations of astrocytes can be labeled in slice preparations of nervous tissue by particle-mediated ballistic delivery of lipophilic carbocyanine dyes such as DiI, DiO, and DiD ("DiOlistic" labeling) (Gan and others 2000; Benediktsson and others 2005). The basic principle is to shoot gold or tungsten particles coated with the lipophilic dyes into the tissue, which then penetrate the cells. The force for the particle acceleration comes from high-pressure helium. This technique is similar to that used for gene transfection (Lo and others 1994). Using carbocynanine dyes, the labeling involves passive dye transfer and diffusion along the cell membrane, revealing the entire morphology of the astrocyte. Living or fixed tissue can be labeled rapidly by many different colors at low or very high densities.

Transgenic Mice

Transgenic mice have been developed in which proteins found in astrocytes (e.g., GFAP, nestin, S100β) are used to target reporter molecules such as GFP. Recent studies have performed large-scale genetic analysis on the astrocyte transcriptome to identify molecules that are particularly abundant in astrocytes and thus differentiate them from other glia and neurons (Lovatt and others 2007; Cahoy and others 2008). Such studies have revealed molecular markers that may better label a greater proportion of the astrocyte population compared to GFAP. One candidate is the protein Aldh1L1 (Cahoy and others 2008). Table 1 shows some of the transgenic mouse strains available that have GFP-expressing astrocytes.

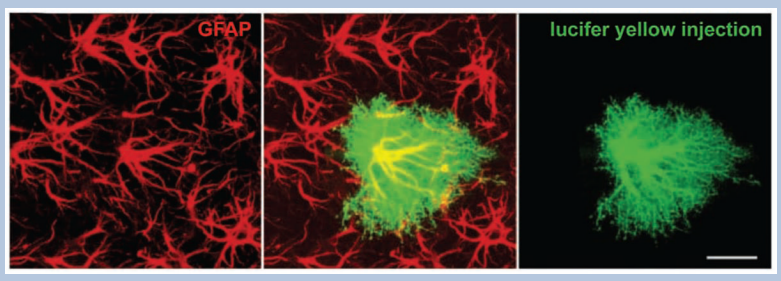

Dye-filling individual astrocytes with lucifer yellow shows the many fine processes that are not visualized by labeling with a GFAP antibody. GFAP-containing intermediate filaments are abundant in the main processes of the astrocyte but not detectable in the fine and terminal processes. Scale bar = 20 μm. Adapted from Wilhelmsson and others (2004).

Table 1

Transgenic Mouse Strains with GFP-Expressing Astrocytes

Reference	Promoter	Reporter
Nolte and others (2001)	Human GFAP	EGFP
Zhuo and others (1997)	Human GFAP	hGFP-S65T
Suzuki and others (2003)	Mouse GFAP	EGFP
Livet and others (2007)	Stochastic	Various
Yamaguchi and others (2000)	Rat nestin	EGFP
Vives and others (2003)	Mouse S100β	EGFP
Heintz (2004); Doyle and others (2008)	BAC-Aldh1L1	EGFP
Regan and others (2007)	BAC-GLT1	EGFP

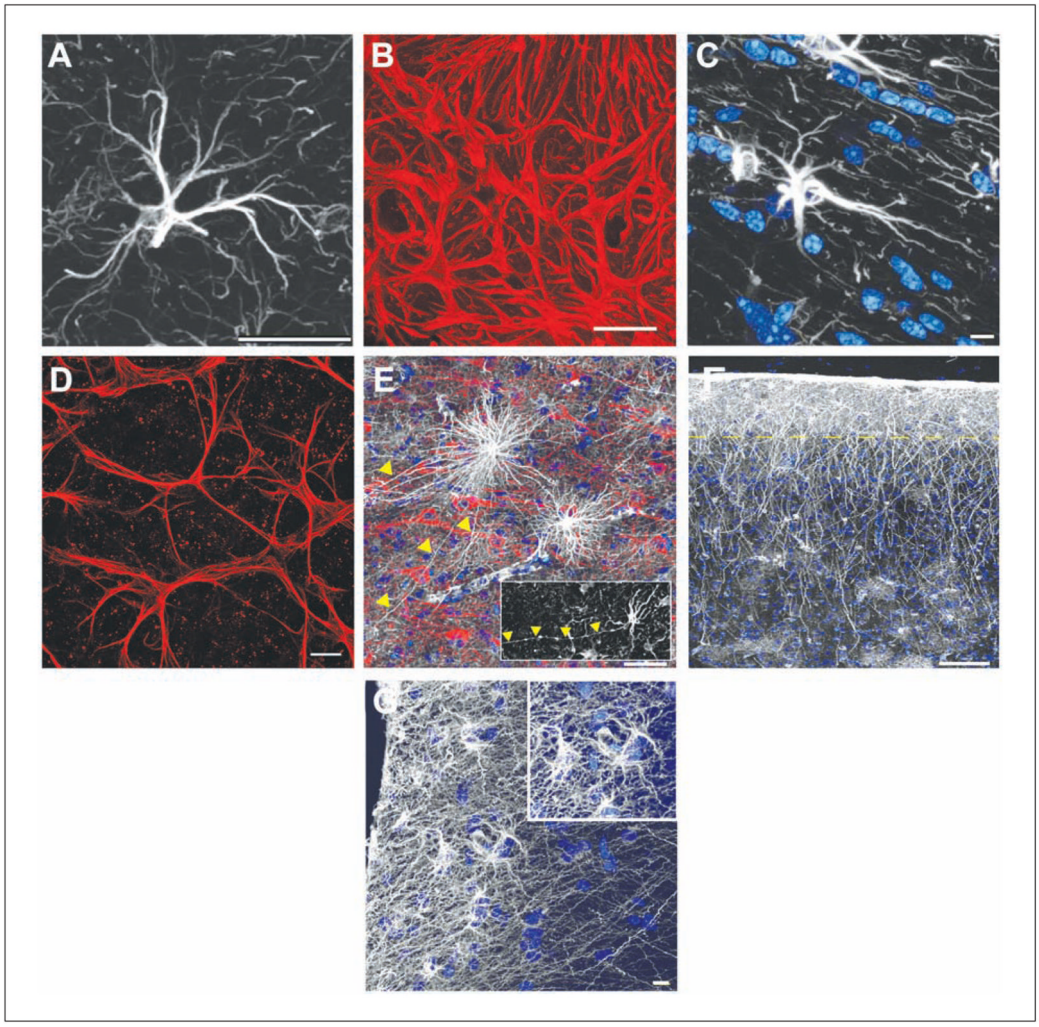

Figure 1.
The various morphologies of GFAP-labeled astrocytes. (A) A typical mouse protoplasmic astrocyte demonstrating the stellate morphology. Scale bar = 20 μm. (B) The processes of astrocytes within the optic nerve head overlap and form a dense meshwork. The boundaries between neighboring astrocytes are not visible. Scale bar = 20 μm. (C) A typical mouse fibrous astrocyte in the white matter. Nuclear stain, blue. Scale bar = 10 μm. (D) The processes of astrocytes within the mouse retina overlap. Similar to the optic nerve, it is not clear where the boundaries of an astrocyte lie. Scale bar = 20 μm. (E) Varicose projection astrocytes reside in layers 5 to 6 of the human cortex and extend long processes characterized by evenly spaced varicosities. Inset: A varicose projection astrocyte from a chimpanzee cortex. Scale bar = 50 μm. (F) Primate-specific interlaminar astrocytes occupy layer 1 of the cortex. Yellow dotted line indicates the border between layers 1 and 2. Scale bar = 100 μm. (G) High-power image of layer 1 showing interlaminar astrocytes. Inset: The cell bodies. Scale bar = 10 μm. Panels A, C, E, F, and G adapted from Oberheim and others (2009).

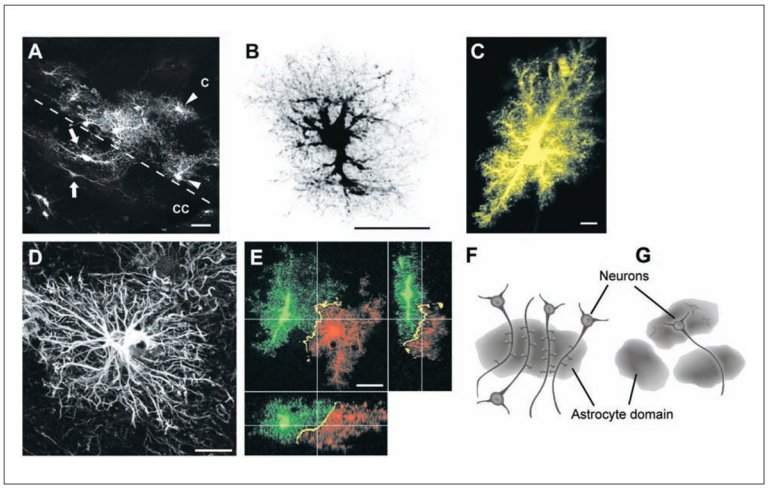

Figure 2.

(A) Protoplasmic astrocytes in the cortex (C) of the hGFAPpr-EGFP mouse lying adjacent to fibrous astrocytes in the corpus callosum (CC). Although both types of astrocytes appear similar when labeled with GFAP, they are morphologically distinct when their complete morphology is visualized. Scale bar = 20 μm. (B) A dye-filled protoplasmic astrocyte from the hippocampus, revealing the fine spongiform processes. Scale bar = 25 μm. (C) Protoplasmic astrocytes in CA1 stratum radiatum are fusiform in shape, rather than spherical, as in the cortex. Scale bar = 10 μm. (D) A typical GFAP-labeled human protoplasmic astrocyte. These astrocytes are larger and more complex than in the mouse. Scale bar = 20 μm. (E) Neighboring protoplasmic astrocytes organize themselves in nonoverlapping spatial domains, with minimal overlap of their most peripheral processes. Scale bar = 20 μm. (F) A diagram illustrating the concept of functional synaptic islands. A group of dendrites from several neurons are enwrapped by a single astrocyte. Synapses within the territory of this astrocyte have the potential to be modulated in a coordinated manner by gliotransmitters released from this astrocyte. (G) A diagram showing the domains of three astrocytes. A single neuron may extend its processes into the domain of another astrocyte, pointing to the potential of different neuronal compartments being modulated by different astrocytes. Panels B and E adapted from Wilhelmsson and others (2006). Panel C adapted from Oberheim and others (2009). Panel D adapted from Bushong and others (2002). Panels F and G adapted from Halassa and others (2007).

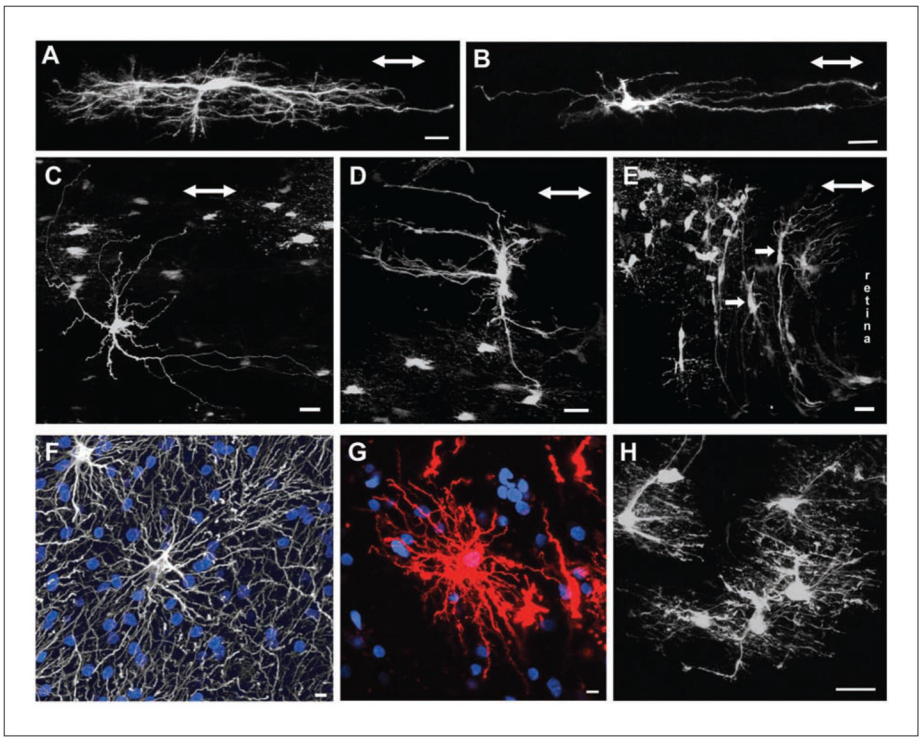

Figure 3.

(A) Longitudinally oriented fibrous astrocyte from the myelinated region of the hGFAPpr-EGFP optic nerve. In this example, the processes are “hairy” with many fine branches. Scale bar = 20 μm. (B) Another example of a fibrous astrocyte from the myelinated optic nerve. This astrocyte is less complex and has smoother processes. Scale bar = 20 μm. (C) An example of a randomly oriented fibrous astrocyte. These astrocytes have processes extending both longitudinally and transversely to the long axis of the nerve. Scale bar = 20 μm. (D) An example of a transversely oriented fibrous astrocyte. Scale bar = 20 μm. (E) The optic nerve head consists predominantly of transversely oriented astrocytes with thick elongated cell bodies and primary processes extending long distances (arrows). These astrocytes have very few processes extending in parallel to the long axis of the nerve. Scale bar = 20 μm. (F) A human fibrous astrocyte in the white matter labeled with GFAP. Nuclear stain, blue. Scale bar = 10 μm. (G) Human fibrous astrocyte labeled with DiI, revealing the full structure of the cell. DiI, red. Nuclear stain, blue. Scale bar = 10 μm. (H) The processes of neighboring fibrous astrocytes overlap extensively. Scale bar = 20 μm. The double-headed arrow in panels A to E represents the direction of the long axis of the optic nerve. Panels A and H adapted from Sun and others (2010). Panels B, D, and E adapted from Sun and others (2009). Panels F and G adapted from Oberheim and others (2009).

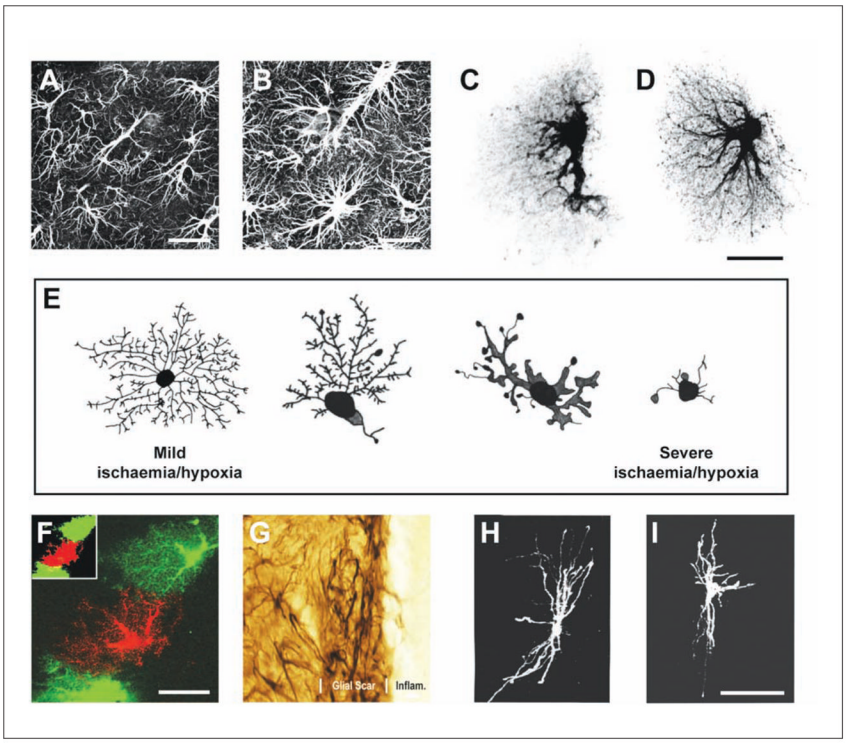

Figure 4.

(A) Antibodies against GFAP label the intermediate filaments predominantly found in the soma and the main processes of astrocytes. Scale bar = 25 μm. (B) Reactive astrocytes up-regulate the expression of GFAP, demonstrating hypertrophy of the cell bodies and processes. Scale bar = 25 μm. (C) A dye-filled astrocyte from the hippocampus, revealing the spongiform nature of these cells. (D) Reactive protoplasmic astrocytes undergo hypertrophy of the cell body and processes and increase the number of main processes leaving the soma and the number of fine branches. Scale bar = 25 μm. (E) A schematic showing ischemia/hypoxia induces a different morphological change in cortical astrocytes. As the severity of the insult increases, there is increased hypertrophy and a decrease in the complexity of the branching pattern. (F) Neighboring reactive protoplasmic astrocytes maintain nonoverlapping spatial domains. Scale bar = 25 μm. (G) The reaction of astrocytes to insult is spatially distinct. Reactive astrocytes immediately adjacent to a lesion have processes that overlap extensively and interdigitate, forming a distinct boundary around the lesion. Scale bar = 8 μm. (H) A typical transverse oriented fibrous astrocyte from the rat optic nerve. (I) Reactive fibrous astrocytes remodel differently from protoplasmic astrocytes. Unlike protoplasmic astrocytes, astrocytes in the myelinated optic nerve show a reduction in the number of processes and branchings, a thickening of remaining processes, and a withdrawal of radial processes ending at the glia limitans. This reduces the overall complexity of the branching structure. Scale bar = 50 μm. Panels A to D and F adapted from Wilhelmsson and others (2006). Panel E adapted from Sullivan and others (2010). Panel G adapted from Sofroniew (2009). Panels H and I adapted from Butt and Colquhoun (1996).

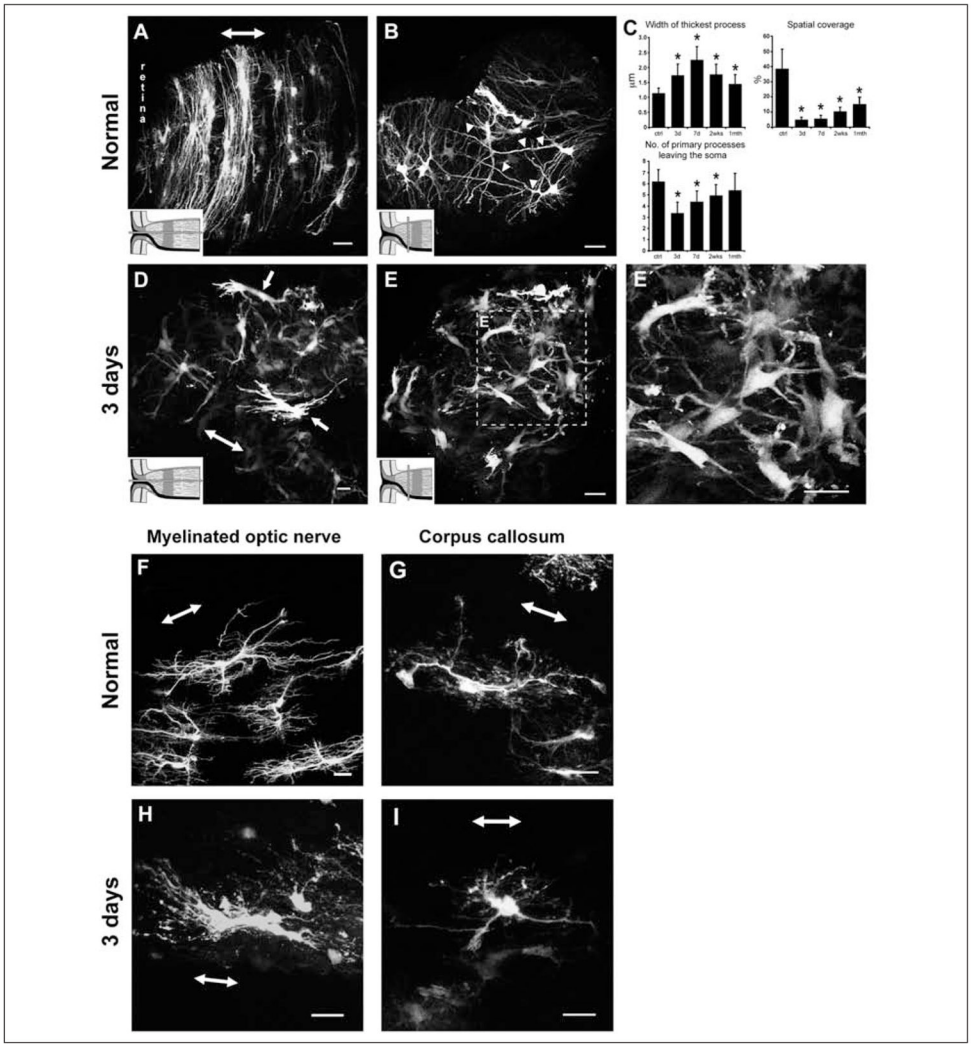

Figure 5.

Normal and reactive fibrous astrocytes in the optic nerve head, myelinated optic nerve, and corpus callosum of the hGFAPpr-EGFP mouse. (A) Normal astrocytes in the optic nerve head have processes that are transversely arranged to form a sheet-like arrangement. (B) They have long primary processes that traverse the entire width of the optic nerve to contact the pial wall (arrowheads). The processes of neighboring astrocytes overlap extensively. (C) Quantitative analysis of changes in the morphological parameters after an optic nerve crush. (D) At 3 days after nerve crush, astrocytes become reactive, show hypertrophy of the soma and processes, and lose their transverse orientation. (E–E′) They retract their primary and higher order processes. The shortening of processes reduces the spatial coverage of individual astrocytes. (F) Longitudinally oriented astrocytes in the myelinated optic nerve were hairy in appearance, with many small fine processes projecting from the primary processes. (G) Astrocytes in the corpus callosum were similar in appearance to those in the myelinated optic nerve. Their main processes run in parallel to the nerve fibers. (H, I) Three days after crush, these astrocytes showed changes similar to those for reactive astrocytes in the optic nerve head: hypertrophy of the soma and remaining processes and retraction of their primary and higher order processes. The schematic in panels A, B, D, and E depicts how the optic nerve was sectioned (gray bars). The double-headed arrow in some panels

indicates the direction of the long axis of the optic nerve. Scale bar in all panels = 20 μm. All panels adapted from Sun and others (2010).

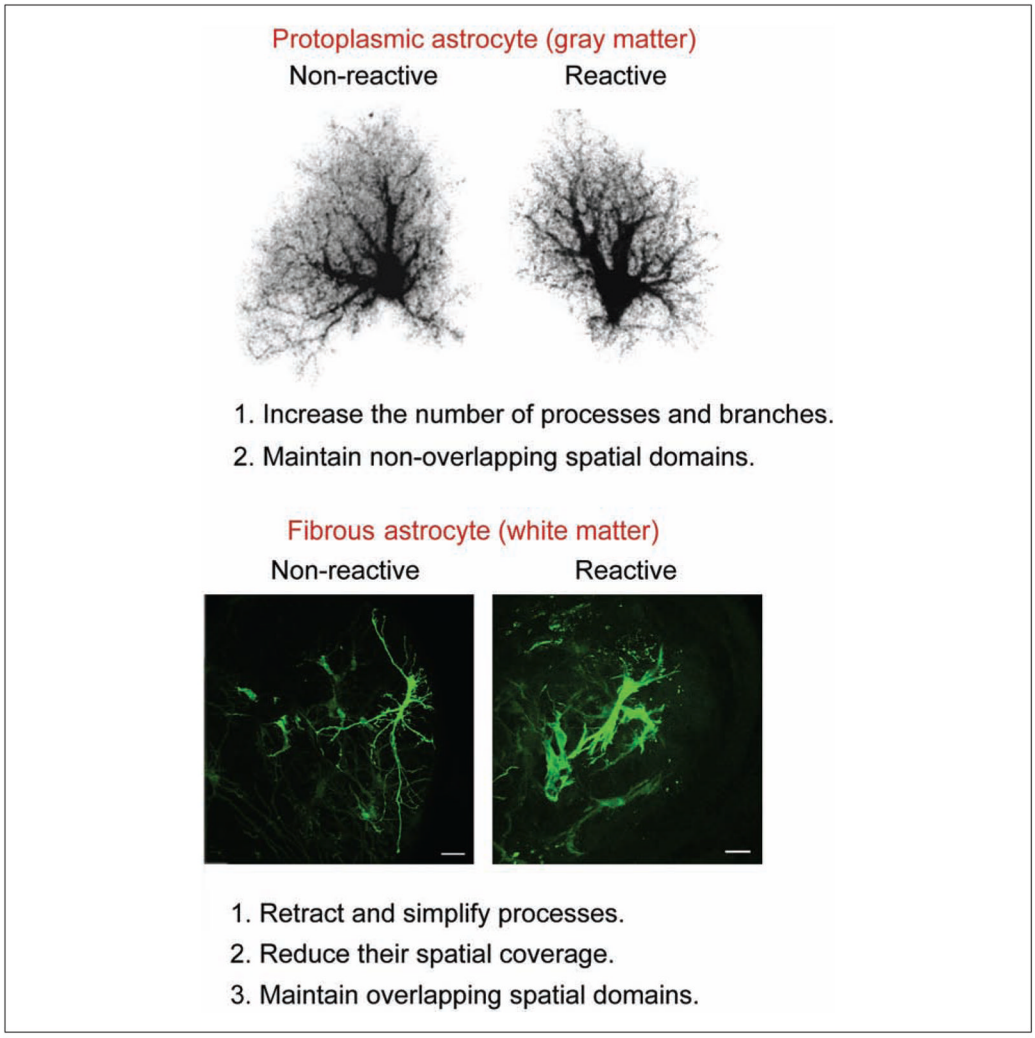

Figure 6.
Fibrous astrocytes react very differently to protoplasmic astrocytes following mechanical injury. Although both types of astrocytes undergo hypertrophy of the cell bodies and processes, fibrous astrocytes retract and simplify their branching structure. Scale bar = 20 μm.

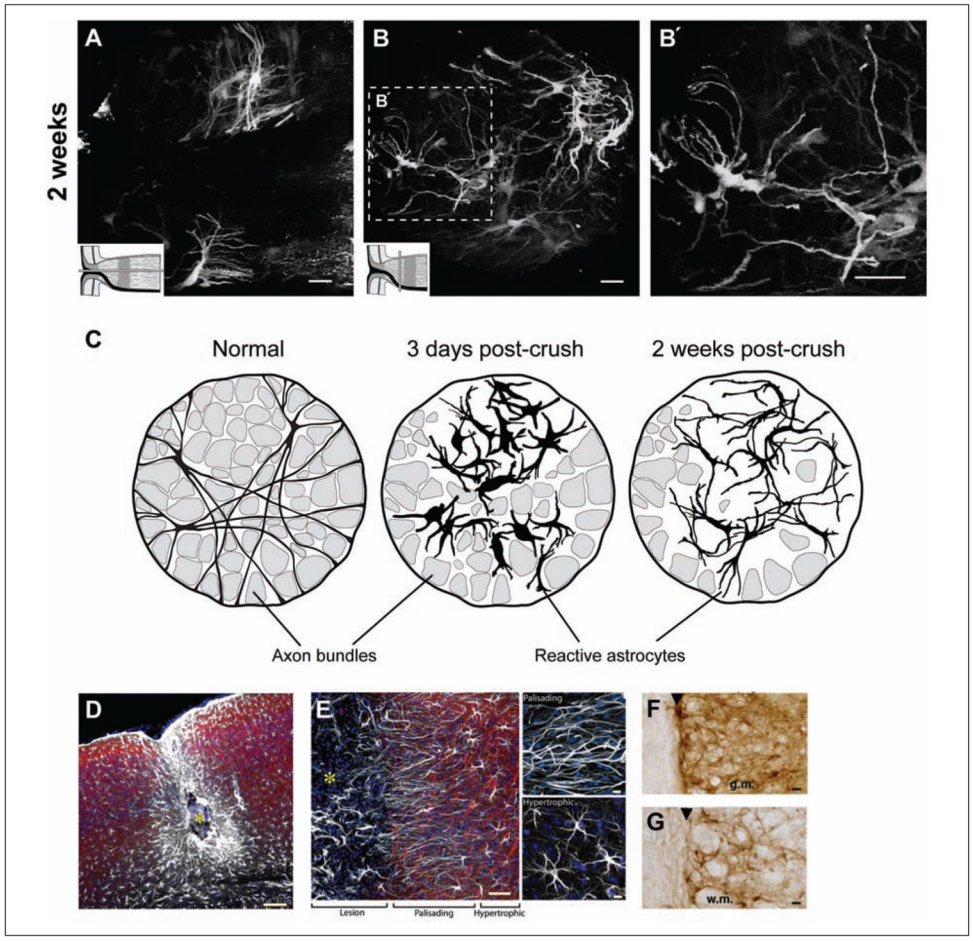

Figure 7.

Reactive fibrous astrocytes from the optic nerve head of the hGFAPpr-EGFP mouse 2 weeks after nerve crush. Longitudinal (A) and transverse (B–B′) sections show that by 2 weeks after nerve crush, the morphology of astrocytes has returned to a near normal appearance. There was thinning and re-extension of many of the processes compared to 3 days (see Fig. 5D–5E′), although they never recover their original length. The processes follow a tortuous path and do not form glial tubes. The schematic in A and B depicts how the optic nerve was sectioned (gray bars). Scale bar in panels A to B′ = 20 μm. (C) Schematic representation of the two-stage remodeling process of reactive astrocytes within the glial lamina. Fibrous astrocytes initially respond by hypertrophy of the soma and proximal processes and retraction of the distal ones. This reduces their spatial domain and disrupts the organization of the glial tubes. By 2 weeks after crush, the processes have re-extended, and their thickness is reduced. (D) The site of injury after ferrous chloride injection. The center of the lesion (yellow asterisk) is surrounded by palisading astrocytes and, at a greater distance, by hypertrophic astrocytes. Scale bar = 100 μm. (E) High-power image of the border of an injury site. Palisading astrocytes directly adjacent to the lesion extend long processes oriented toward the lesion site (<200 μm). Their processes overlap extensively. Hypertrophic astrocytes (200–1000 μm) displayed less pronounced reactive changes, and their processes were not oriented towards the lesion site. Scale bar = 50 μm. Scale bar in top and bottom right panels = 10 μm. (F) The boundary zone in the gray matter (g.m.) of a spinal cord lesion showing the demarcation formed by an organized scar (black arrowhead). The processes of β-gal–stained astrocytes overlap extensively within 100 μm of the lesion.

Scale bar = 30 μm. (G) A similar zone in the white matter (w.m.) of a spinal cord lesion. Here too, processes of neighboring astrocytes overlap. Scale bar = 30 μm. Panels A to C adapted from Sun and others (2010). Panels D and E adapted from Oberheim and others (2008). Panels F and G adapted from Herrmann and others (2008).

Table 2

Dimensions of Normal Protoplasmic and Fibrous Astrocytes as Measured by Different Labeling Techniques

	Mouse		Human	Chimpanzee
	Particle-mediated dye labeling	**GFAP labeling**	**GFAP labeling**	**GFAP labeling**
Protoplasmic (cortical)				
Diameter, μm	57.7 ± 3.8	56.0 ± 2.0	142.6 ± 5.8	81.7 ± 1.9
Longest process, μm	39.8 ± 2.3	37.2 ± 1.2	97.9 ± 5.2	—
Thickest process, μm	2.6 ± 0.2	2.2 ± 0.1	2.9 ± 0.18	—
No. of GFAP+ processes	—	3.75 ± 0.11	37.5 ± 5.17	—
Fibrous (corpus callosum)				
Diameter, mm	—	85.6 ± 2.7	183.2 ± 6.1	—

Data derived from Oberheim and others (2008, 2009).